mental disorders, and diabetes or other metabolic diseases of unknown cause, we plan to conduct research based on the assumption that such cases include those caused by abnormalities in genes identified in MRCD patients.

## Acknowledgements

This work was supported in part by a grant for Innovative Cell Biology by Innovative Technology (Cell Innovation Program) and Support Project from the Ministry of Education, Culture, Sports, Science and Technology (MEXT), Japan, by a grant for Strategic Research Centers in Private Universities from MEXT, Japan to Saitama Medical University Research Center for Genomic Medicine, and by Grants-in-Aid for Research on Intractable Diseases (Mitochondrial Disorder) from the Ministry of Health, Labor and Welfare of Japan. Dr. Murayama was supported by the Kawano Masanori Memorial Public Interest Incorporated Foundation for Promotion of Pediatrics. The authors would also like to thank Dr. Ayako Fujinami, Dr. Kaori Muta, Dr. Emi Kawachi, Dr. Takuya Fushimi, Dr. Keiko Ichimoto, Dr. Tomoko Tsuruoka, Ms. Keio Baba and Ms. Masami Ajima at Chiba Children's Hospital for their support.

## References

[1] D. Skladal, J. Halliday, D.R. Thorburn, Minimum birth prevalence of mitochondrial respiratory chain disorders in children, Brain 126 (2003) 1905–1912.
[2] S. Dimauro, G. Davidzon, Mitochondrial DNA and disease, Ann. Med. 37 (2005) 222–232.
[3] D.M. Kirby, D.R. Thorburn, Approaches to finding the molecular basis of mitochondrial oxidative phosphorylation disorders, Twin Res. Hum. Genet. 11 (2008) 395–411.
[4] D.C. Wallace, Mitochondria and cancer, Nat. Rev. Cancer 12 (2012) 685–698.
[5] M.F. Lopez, B.S. Kristal, E. Chernokalskaya, A. Lazarev, A.I. Shestopalov, A. Bogdanova, M. Robinson, High-throughput profiling of the mitochondrial proteome using affinity fractionation and automation, Electrophoresis 21 (2000) 3427–3440.
[6] H. Schägger, K. Pfeiffer, The ratio of oxidative phosphorylation complexes I–V in bovine heart mitochondria and the composition of respiratory chain supercomplexes, J. Biol. Chem. 276 (2001) 37861–37867.
[7] D.R. Thorburn, Mitochondrial disorders: prevalence, myths and advances, J. Inherit. Metab. Dis. 27 (2004) 349–362.
[8] W.J. Koopman, P.H. Willems, J.A. Smeitink, Monogenic mitochondrial disorders, N. Engl. J. Med. 366 (2012) 1132–1141.
[9] S.B. Vafai, V.K. Mootha, Mitochondrial disorders as windows into an ancient organelle, Nature 491 (2012) 374–383.
[10] E.J. Tucker, A.G. Compton, D.R. Thorburn, Recent advances in the genetics of mitochondrial encephalopathies, Curr. Neurol. Neurosci. Rep. 10 (2010) 277–285.
[11] D.M. Kirby, M. Crawford, M.A. Cleary, H.H. Dahl, X. Dennett, D.R. Thorburn, Respiratory chain complex I deficiency: an underdiagnosed energy generation disorder, Neurology 52 (1999) 1255–1264.
[12] F.P. Bernier, A. Boneh, X. Dennett, C.W. Chow, M.A. Cleary, D.R. Thorburn, Diagnostic criteria for respiratory chain disorders in adults and children, Neurology 59 (2002) 1406–1411.
[13] H. Schägger, G. von Jagow, Blue native electrophoresis for isolation of membrane protein complexes in enzymatically active form, Anal. Biochem. 199 (1991) 223–231.
[14] K. Gibson, J.L. Halliday, D.M. Kirby, J. Yaplito-Lee, D.R. Thorburn, A. Boneh, Mitochondrial oxidative phosphorylation disorders presenting in neonates: clinical manifestations and enzymatic and molecular diagnoses, Pediatrics 122 (2008) 1003–1008.
[15] T. Yamazaki, K. Murayama, A.G. Compton, C. Sugiana, H. Harashima, S. Amemiya, M. Ajima, T. Tsuruoka, A. Fujinami, E. Kawachi, Y. Kurashige, K. Matsushita, H. Wakiguchi, M. Mori, H. Iwasa, Y. Okazaki, D.R. Thorburn, A. Ohtake, Molecular diagnosis of mitochondrial respiratory chain disorders in Japan: focusing on mitochondrial DNA depletion syndrome, Pediatr. Int. 56 (2014)(in press).
[16] C. Gilissen, A. Hoischen, H.G. Brunner, J.A. Veltman, Disease gene identification strategies for exome sequencing, Eur. J. Hum. Genet. 20 (2012) 490–497.
[17] H. Li, R. Durbin, Fast and accurate short read alignment with Burrows–Wheeler transform, Bioinformatics 25 (2009) 1754–1760.
[18] S.B. Ng, E.H. Turner, P.D. Robertson, S.D. Flygare, A.W. Bigham, C. Lee, T. Shaffer, M. Wong, A. Bhattacharjee, E.E. Eichler, M. Bamshad, D.A. Nickerson, J. Shendure, Targeted capture and massively parallel sequencing of 12 human exomes, Nature 461 (2009) 272–276.
[19] A. McKenna, M. Hanna, E. Banks, A. Sivachenko, K. Cibulskis, A. Kernytsky, K. Garimella, D. Altshuler, S. Gabriel, M. Daly, M.A. DePristo, The Genome Analysis Toolkit: a MapReduce framework for analyzing next-generation DNA sequencing data, Genome Res. 20 (2010) 1297–1303.
[20] K. Wang, M. Li, H. Hakonarson, ANNOVAR: functional annotation of genetic variants from high-throughput sequencing data, Nucleic Acids Res. 38 (2010) e164.
[21] X. Liu, X. Jian, E. Boerwinkle, dbNSFP: a lightweight database of human nonsynonymous SNPs and their functional predictions, Hum. Mutat. 32 (2011) 894–899.
[22] M. Yandell, C. Huff, H. Hu, M. Singleton, B. Moore, J. Xing, L.B. Jorde, M.G. Reese, A probabilistic disease-gene finder for personal genomes, Genome Res. 21 (2011) 1529–1542.
[23] The UniProt Consortium, Update on activities at the Universal Protein Resource (UniProt) in 2013, Nucleic Acids Res. 41 (2013) D43–D47.
[24] D.J. Pagliarini, S.E. Calvo, B. Chang, S.A. Sheth, S.B. Vafai, S.E. Ong, G.A. Walford, C. Sugiana, A. Boneh, W.K. Chen, D.E. Hill, M. Vidal, J.G. Evans, D.R. Thorburn, S.A. Carr, V.K. Mootha, A mitochondrial protein compendium elucidates complex I disease biology, Cell 134 (2008) 112–123.

CLINICAL REPORT

AMERICAN JOURNAL OF medical genetics PART A

# Compound Heterozygous Deletions in Pseudoautosomal Region 1 in an Infant With Mild Manifestations of Langer Mesomelic Dysplasia

**Takayoshi Tsuchiya,[1,2] Minoru Shibata,[3] Hironao Numabe,[3,4] Tomoko Jinno,[1] Kazuhiko Nakabayashi,[5] Gen Nishimura,[6] Toshiro Nagai,[2] Tsutomu Ogata,[1,7] and Maki Fukami[1]***

[1]Department of Molecular Endocrinology, National Research Institute for Child Health and Development, Tokyo, Japan

[2]Department of Pediatrics, Dokkyo Medical University Koshigaya Hospital, Koshigaya, Japan

[3]Department of Pediatrics, Kyoto University Hospital, Kyoto, Japan

[4]Graduate School of Humanities and Sciences, Ochanomizu University, Tokyo, Japan

[5]Department of Maternal-Fetal Biology, National Research Institute for Child Health and Development, Tokyo, Japan

[6]Department of Pediatric Imaging, Tokyo Metropolitan Children's Medical Center, Tokyo, Japan

[7]Department of Pediatrics, Hamamatsu University School of Medicine, Hamamatsu, Japan

Manuscript Received: 15 May 2013; Manuscript Accepted: 13 September 2013

Haploinsufficiency of *SHOX* on the short arm pseudoautosomal region (PAR1) leads to Leri–Weill dyschondrosteosis (LWD), and nullizygosity of *SHOX* results in Langer mesomelic dysplasia (LMD). Molecular defects of LWD/LMD include various microdeletions in PAR1 that involve exons and/or the putative upstream or downstream enhancer regions of *SHOX*, as well as several intragenic mutations. Here, we report on a Japanese male infant with mild manifestations of LMD and hitherto unreported microdeletions in PAR1. Clinical analysis revealed mesomelic short stature with various radiological findings indicative of LMD. Molecular analyses identified compound heterozygous deletions, that is, a maternally inherited ~46 kb deletion involving the upstream region and exons 1–5 of *SHOX*, and a paternally inherited ~500 kb deletion started from a position ~300 kb downstream from *SHOX*. In silico analysis revealed that the downstream deletion did not affect the known putative enhancer regions of *SHOX*, although it encompassed several non-coding elements which were well conserved among various species with *SHOX* orthologs. These results provide the possibility of the presence of a novel enhancer for *SHOX* in the genomic region ~300 to ~800 kb downstream of the start codon.



**Key words:** *SHOX*; langer mesomelic dysplasia; deletion; enhancer

**How to Cite this Article:**
Tsuchiya T, Shibata M, Numabe H, Jinnno T, Nakabayashi K, Nishimura G, Nagai T, Ogata T, Fukami M. 2014. Compound heterozygous deletions in pseudoautosomal region 1 in an infant with mild manifestations of langer mesomelic dysplasia.
Am J Med Genet Part A 164A:505–510.

## INTRODUCTION

*SHOX* on the short arm pseudoautosomal region (PAR1) is a transcription factor gene exclusively expressed in the developing limbs and pharyngeal arches [Rao et al., 1997; Clement-Jones et al., 2000]. Haploinsufficiency of *SHOX* leads to idiopathic short stature and Leri–Weill dyschondrosteosis (LWD; OMIM #127300), and nullizygosity of *SHOX* results in Langer mesomelic dysplasia (LMD; OMIM #249700) [Rao et al., 1997; Belin et al., 1998; Shears et al., 1998; Zinn et al., 2002]. Previous studies in patients with LWD and LMD have identified several copy-number abnormalities in PAR1 that involved coding exons and/or the putative upstream or downstream enhancer regions, together with multiple point

We declare no potential conflicts of interest relevant to this article.
Grant sponsor: Ministry of Health, Labor and Welfare; Grant sponsor: Ministry of Education, Culture, Sports, Science and Technology; Grant sponsor: National Center for Child Health and Development; Grant sponsor: Takeda Science Foundation; Grant sponsor: Daiichi-Sankyo Foundation of Life Science.

*Correspondence to:
Maki Fukami, Department of Molecular Endocrinology, National Research Institute for Child Health and Development, 157-8535 Tokyo, Japan.
E-mail: fukami-m@ncchd.go.jp

Article first published online in Wiley Online Library (wileyonlinelibrary.com): 5 December 2013
DOI 10.1002/ajmg.a.36284

mutations in the coding region [Rao et al., 1997; Belin et al., 1998; Shears et al., 1998; Benito-Sanz et al., 2005, 2011, 2012b; Fukami et al., 2005, 2006; Bertorelli et al., 2007; Sabherwal et al., 2007; Chen et al., 2009; Durand et al., 2010]. The putative enhancers of *SHOX* have been mapped to a ~300 kb region ~95 kb upstream, and to a ~30 kb region ~250 kb downstream from the start codon [Benito-Sanz et al., 2005, 2012a,b; Fukami et al., 2006]. The putative downstream enhancer region contains several conserved non-coding elements (CNEs) that exert enhancer activity in the developing chicken limb bud [Sabherwal et al., 2007] and in human osteosarcoma cells [Fukami et al., 2006; Benito-Sanz et al., 2012b]. Since molecular abnormalities have not been detected in a substantial portion of patients with LWD/LMD [Zinn et al., 2002; Fukami et al., 2008; Rosilio et al., 2012], it appears that unknown genetic or environmental factors are also involved in the development of these conditions.

The clinical severity of SHOX abnormalities is highly variable [Binder, 2011]. Relatively severe phenotypes in adult female patients indicate that gonadal estrogens enhance skeletal abnormalities in SHOX abnormalities [Ogata et al., 2001; Binder, 2011]. However, there may be other phenotypic modulators for this condition [Binder et al., 2004]. Here, we report on a male infant with mild LMD phenotype and compound heterozygosity of hitherto unreported microdeletions in PAR1.

## CLINICAL REPORT

This Japanese male infant was a dizygotic twin conceived by in vitro fertilization. At 24 weeks gestation, an ultrasound examination delineated short extremities in one fetus and a normal skeletal appearance in the other. At 27 weeks gestation, caesarean section was performed because of bradycardia in both fetuses. At birth, the patient presented with a mesomelic appearance with a body length of 33.5 cm (−1.1 SD), weight of 1,130 g (+0.4 SD), and head circumference of 26.5 cm (+1.0 SD). His twin brother was normally proportioned with body length 35.5 cm (−0.1 SD), weight 854 g (−1.5 SD), and head circumference 25.0 cm (±0 SD). Bone survey of the patient at 2 months of age showed markedly curved radii, hypoplastic ulnas and fibulas, and metaphyseal splaying (Fig. 1A). The patient and his brother received standard medical interventions for prematurity, and were discharged from hospital at 3 months of age.

On his latest visit at 21 months of age, the infant manifested obvious mesomelic short stature with a height of 69.3 cm (−3.9 SD), weight of 8.0 kg (−2.7 SD), and head circumference of 46.6 cm (−1.0 SD; Fig. 1B). His developmental milestones were almost normal. His brother had a proportionate short stature with a height of 74.1 cm (−2.6 SD), weight of 8.5 kg (−2.3 SD), and head circumference of 46.2 cm (−1.3 SD). The mother showed limited movement of the wrist and mesomelic short stature (140 cm, −3.6 SD), while the father was clinically normal and had a normal height (165 cm, −1.0 SD). Radiological examinations were not performed for the parents or brother.

## MOLECULAR ANALYSES

This study was approved by the Institutional Review Board Committee at the National Center for Child Health and Development.

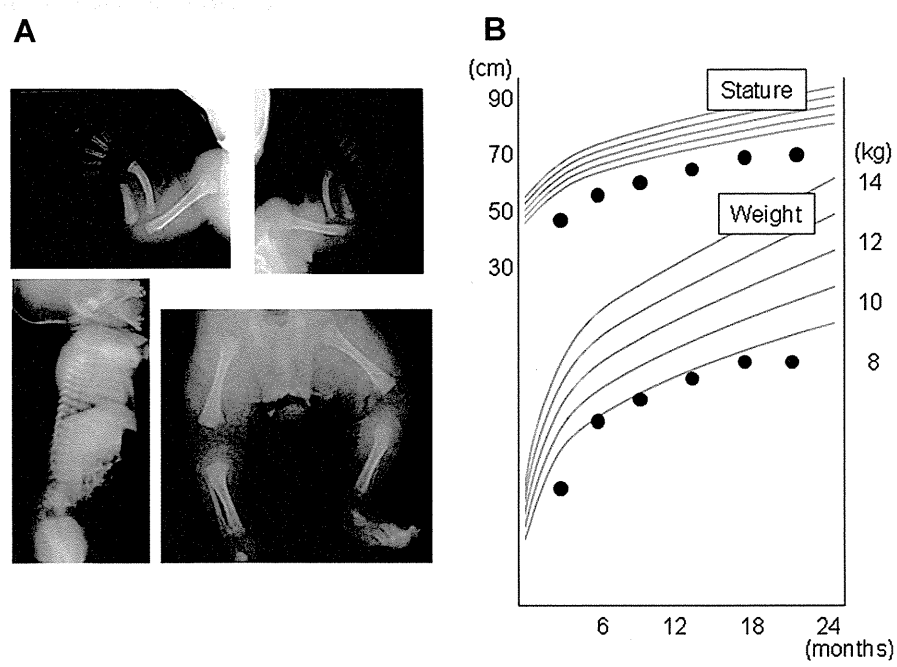


**FIG. 1. Clinical findings of the infant. A: X-Ray at 10 weeks of age. Markedly curved radii, hypoplastic ulnas and fibulas, and metaphyseal splaying are shown. B: Growth pattern. Height and weight of the infant are plotted on the longitudinal height and weight standards for Japanese boys (the mean, ±1.0 SD and ±2.0 SD, respectively).**

After taking written informed consent from the parents, leukocyte genomic DNA samples were obtained from the infant and parents. First, we performed direct sequencing analysis for *SHOX* by a previously described method [Shears et al., 1998]. No nucleotide alterations in the coding exons were identified in the infant. Next, we performed multiplex ligation-dependent probe amplification (MLPA) using a SALSA MLPA Kit (P018 SHOX-F1, MRC-Holland, Amsterdam, the Netherlands). Two heterozygous deletions in PAR1 were identified in the infant; a deletion involving exons 1–5 of *SHOX*, and a deletion affecting the downstream region of *SHOX* that corresponds to four MLPA probes from 05649-L20176 to 13911-L19678 (Fig. 2). Then, we examined the extent of the deletions by comparative genomic hybridization (CGH) using a custom-built oligo-microarray harboring 26,274 probes for PAR1 and several reference probes for other chromosomal regions (4 × 180 K format, Agilent Technologies, Palo Alto, CA; Fig. 3A). The telomeric deletion included a ~46 kb genomic interval (ChrX: 556,720–603,222; hg 19, Build 37) affecting *SHOX* exons 1–5 and a ~28 kb region at the 5′ side of exon 1. The centromeric deletion encompassed a ~500 kb interval (ChrX: 881,006–1,387,599) and started at a point ~300 kb from the start codon of *SHOX*. In silico analysis using UCSC Genome Browser (http://genome.ucsc.edu/) and rVista 2.0 (http://rvista.dcode.org/) revealed that the deletions did not affect the putative upstream or downstream enhancer regions of *SHOX*, and that the downstream deletion encompassed a gene for cytokine receptor-like factor 2 (*CRLF2*) and several CNEs (Fig. 4). Most of these CNEs were well conserved in fugu, frog, chicken, dog and monkey which preserve orthologs of *SHOX* (*Shox*), as well as in opossum which is likely to preserve *Shox*, and were absent in mouse which lack *Shox* (Ensemble Genome Browser, http://ensembl.org/; Fig. 4). Next, MLPA and CGH were performed on the parental samples. The ~46 and ~500 kb deletions were detected in the mother and father, respectively (Figs. 2 and 3A). Thus, the infant was diagnosed as being compound heterozygous for a maternally inherited ~46 kb deletion on the X chromosome and a paternally inherited ~500 kb deletion on the Y chromosome. The results of MLPA and CGH were confirmed by fluorescence in situ hybridization (FISH). FISH probes for *SHOX* exons 3–5 (probe A) and for a region ~320 kb downstream of *SHOX* (probe B) were generated by PCR using primers 5′-CAGCTCTTCCTCAAATTCTTTCC-3′ and 5′-GTGTCTGTCCCATCTCTGGTATC-3′, and 5′-ATAGTG-CATGGGTATCAGAGGTC-3′ and 5′-GGAAAAAGAGTGGGT-

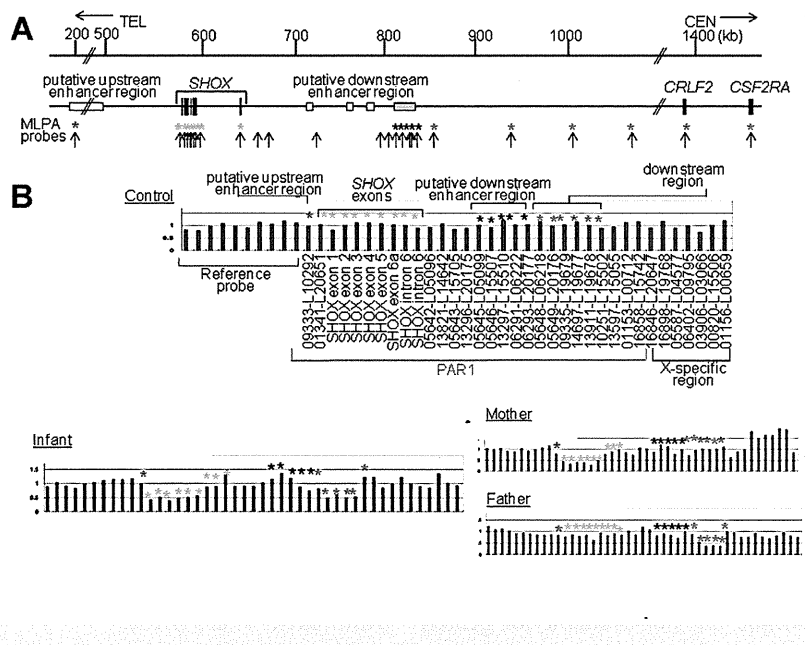


**FIG. 2. Multiplex ligation-dependent probe amplification (MLPA) analysis. A: Schematic representation of the short arm pseudoautosomal region (PAR1). The upper horizontal line indicates the physical distance from the Xp/Yp telomere. Genomic positions refer to the Human Genome (hg 19; NCBI Build 37). The black boxes indicate exons of *SHOX*, *CRLF2*, and *CSF2RA* (not all exons are shown). The white box denotes the putative upstream and downstream enhancer regions (elements) of *SHOX* identified in previous studies [Sabherwal et al., 2007; Benito-Sanz et al., 2012a,b]. The gray box indicates putative downstream enhancer elements that exert enhancer activities in the developing chicken limb [Sabherwal et al., 2007]. Vertical arrows indicate genomic positions of MLPA probes; green asterisks indicate probes for *SHOX* exons, blue and black asterisks indicate probes for the putative upstream and downstream enhancer regions respectively, and red asterisks depict probes for the genomic region between the putative downstream enhancer region and *CSF2RA*. TEL, telomere; CEN, centromere. B: Representative results of MLPA. The asterisks indicate the same probes shown in Fig. 2A. The sample data were normalized to a male sample. Decreased peak heights suggest heterozygous deletions. The infant has two deletions; one involving the upstream region and exons 1–5 of *SHOX*, and the other in the downstream region. The mother and father are heterozygous for the deletions.**

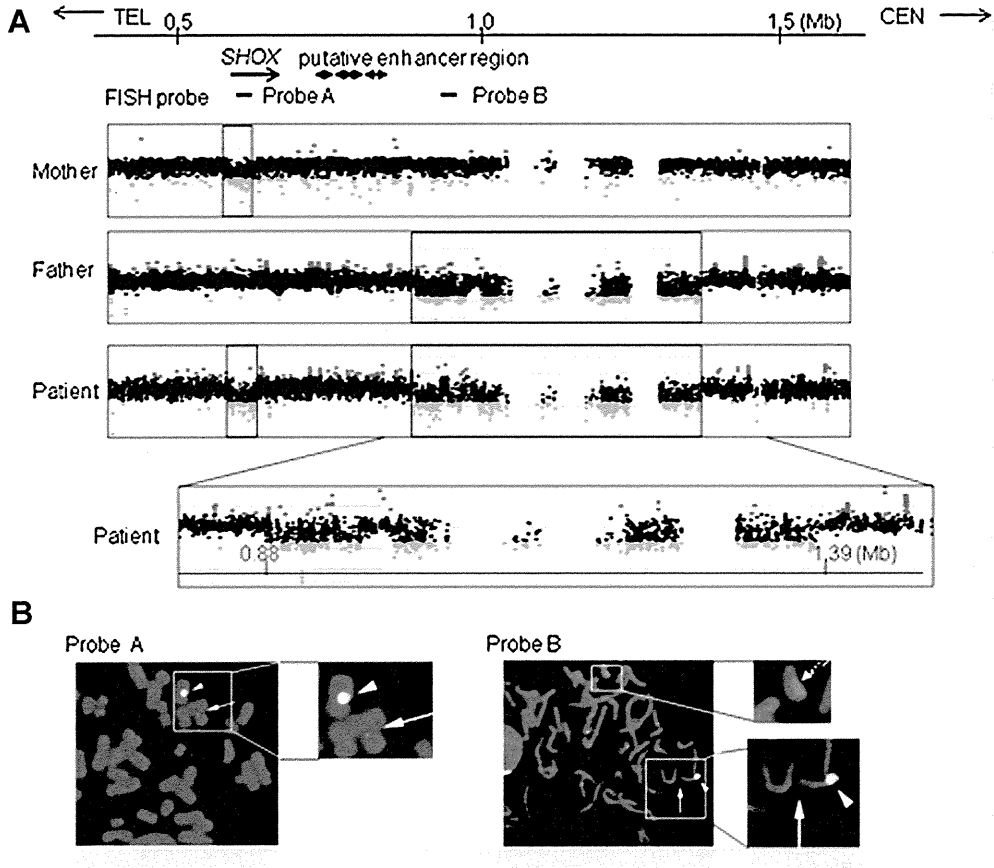


**FIG. 3. Comparative genomic hybridization (CGH) and fluorescence in situ hybridization (FISH) analyses. A: CGH analysis in the infant and his parents. The upper horizontal line indicates physical distance from the Xp/Yp telomere. The genomic position of *SHOX*, the putative downstream enhancer elements, and FISH probes are shown. The black, red, and green dots denote signals indicative of the normal, increased (>+0.5), and decreased (<−0.8) copy numbers, respectively. The blue-shaded boxes indicate deleted regions. B: FISH analyses in the infant. Red signals (arrows) indicate probe A for *SHOX* exons 1–3 and probe B for the *SHOX* downstream region, and green signals (arrow heads) depict *DXZ1* control probes on the X chromosome. Probe A detects a signal on the Y chromosome but not on the X chromosome. Probe B detects a signal on the X chromosome but not on the Y chromosome (a dotted arrow).**

CAGAACTT-3′, respectively. In the infant, probe A detected only one signal on the Y chromosome and probe B detected only one signal on the X chromosome (Fig. 3B).

We attempted to obtain a DNA sample from the twin brother, because he was predicted to carry the same Y chromosomal deletion as the infant. However, the sample was not available for genetic analysis.

## DISCUSSION

We identified compound heterozygous deletions in PAR1 in a male infant. These deletions have not been described previously. The deletion on the X chromosome included most of the coding exons of *SHOX*, and therefore appears to result in complete loss-of-function of the *SHOX* allele. Consistent with this, the mother heterozygous for the same deletion manifested typical clinical features of LWD. In contrast, the deletion on the Y chromosome did not affect exons or the known putative enhancer regions of *SHOX*. Furthermore, this deletion included no genes except *CRLF2*, which has not been implicated in skeletal development [Siracusa et al., 2011]. Clinical examinations of the infant revealed mesomelic short stature and obvious skeletal changes that are more consistent with LMD than with LWD [Fukami et al., 2005; Binder, 2011; Ambrosetti et al., 2013].

Two possible explanations can be made for these results. First, the Y chromosomal deletion in the infant may encompass a hitherto unidentified *cis*-regulatory element of *SHOX*. Recent studies have indicated that several genes such as *SOX9* and *LHX3* have multiple *cis*-acting modules widely distributed around the coding exons [Gordon et al., 2009; Mullen et al., 2012]. Thus, it is possible that coordinated action of multiple regulatory elements is required for adequate *SHOX* expression in the developing limb bud, and that one of such elements is located within the ~500 kb region >300 kb apart from the coding region. Indeed, the Y chromosomal deletion in the infant harbored several CNEs that are well conserved among various species with *SHOX* orthologs.

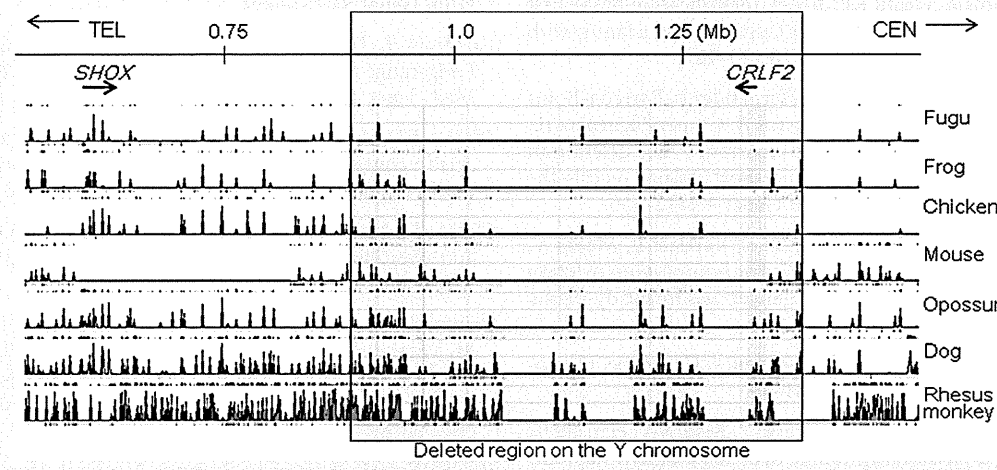


**FIG. 4. Conservation analysis in the short arm pseudoautosomal region of the sex chromosomes (PAR1). The deleted region on the Y chromosome (shaded in gray) contains several non-coding elements that are well conserved in species which preserve *SHOX* orthologs (fugu, frog, chicken, dog, and monkey, and possibly opossum as well) and absent in mouse which lacks an *SHOX* ortholog.**

One of the CNEs in the deletion may be a distal enhancer of *SHOX/Shox*, because CNEs in the human genome frequently exert enhancer activity [Pennacchio et al., 2006]. In this regard, it is noteworthy that the skeletal features of this infant are milder than those of previously reported patients with *SHOX* nullizygosity [Zinn et al., 2002; Fukami et al., 2005; Ambrosetti et al., 2013]; the infant showed no short stature or rhizomelia at birth. Furthermore, the father with the same Y chromosomal deletion manifested no skeletal abnormalities, and the twin brother with possible Y chromosomal deletion showed only mild proportionate short stature. These results can be explained by assuming that deletions involving only the putative enhancer regions exert a relatively mild effect on skeletal growth compared to mutations/deletions affecting the coding exons. Consistent with this, relatively mild LWD phenotypes have been observed in patients with heterozygous downstream deletions [Rosilio et al., 2012], and mild LMD phenotype has been described in a patient with compound heterozygous deletions for *SHOX* exons and the putative downstream enhancer region [Fukami et al., 2005]. Alternatively, *cis*-regulatory deletions may be associated with broad phenotypic variation compared to exonic deletions/mutations, because Chen et al. [2009] have described profound phenotypes in patients with enhancer deletions.

Second, the phenotype of the infant may be explained as an extremely severe manifestation of LWD. If this is the case, the Y chromosomal deletion would be a functionally neutral copy-number variation. The absence of skeletal changes in the father with the Y chromosomal deletion supports this notion. In this regard, previous studies have indicated that phenotypic severities of *SHOX* haploinsufficiency are variable and likely to be affected by multiple factors [Binder et al., 2004; Binder, 2011]. Thus, some genetic or environmental factors may have enhanced the abnormal skeletal formation of this infant with a maternally derived *SHOX* intragenic deletion.

In summary, we identified hitherto unreported deletions in PAR1 in a Japanese infant with a mild LMD phenotype. Further studies will clarify the presence or absence of a novel downstream enhancer of *SHOX* in the genomic region ~300 to ~800 kb from the start codon.

## ACKNOWLEDGMENTS

This work was supported by grants from the following: the Ministry of Health, Labor and Welfare, the Ministry of Education, Culture, Sports, Science and Technology, the National Center for Child Health and Development, the Takeda Science Foundation, and Daiichi-Sankyo Foundation of Life Science.

## REFERENCES

Ambrosetti F, Palicelli A, Bulfamante G, Rivasi F. 2013. Langer mesomelic dysplasia in early fetuses: Two cases and a literature review. Fetal Pediatr Pathol [Epub ahead of print].

Belin V, Cusin V, Viot G, Girlich D, Toutain A, Moncla A, Vekemans M, Le Merrer M, Munnich A, Cormier-Daire V. 1998. SHOX mutations in dyschondrosteosis (Leri–Weill syndrome). Nat Genet 19:67–69.

Benito-Sanz S, Thomas NS, Huber C, Gorbenko del Blanco D, Aza-Carmona M, Crolla JA, Maloney V, Rappold G, Argente J, Campos-Barros A, Cormier-Daire V, Heath KE. 2005. A novel class of pseudoautosomal region 1 deletions downstream of SHOX is associated with Leri–Weill dyschondrosteosis. Am J Hum Genet 77:533–544.

Benito-Sanz S, Barroso E, Heine-Suñer D, Hisado-Oliva A, Romanelli V, Rosell J, Aragones A, Caimari M, Argente J, Ross JL, Zinn AR, Gracia R, Lapunzina P, Campos-Barros A, Heath KE. 2011. Clinical and molecular evaluation of SHOX/PAR1 duplications in Leri–Weill dyschondrosteosis (LWD) and idiopathic short stature (ISS). J Clin Endocrinol Metab 96: E404–E412.

Benito-Sanz S, Aza-Carmona M, Rodríguez-Estevez A, Rica-Etxebarria I, Gracia R, Campos-Barros A, Heath KE. 2012a. Identification of the first PAR1 deletion encompassing upsream SHOX enhancers in a family with idiopathic short stature. Eur J Hum Genet 20:125–127.

Benito-Sanz S, Royo JL, Barroso E, Paumard-Hernández B, Barreda-Bonis AC, Liu P, Gracia R, Lupski JR, Campos-Barros Á, Gómez-Skarmeta JL, Heath KE. 2012b. Identification of the first recurrent PAR1 deletion in Léri–Weill dyschondrosteosis and idiopathic short stature reveals the presence of a novel SHOX enhancer. J Med Genet 49:442–450.

Bertorelli R, Capone L, Ambrosetti F, Garavelli L, Varriale L, Mazza V, Stanghellini I, Percesepe A, Forabosco A. 2007. The homozygous deletion of the 3′ enhancer of the SHOX gene causes Langer mesomelic dysplasia. Clin Genet 72:490–491.

Binder G. 2011. Short stature due to SHOX deficiency: Genotype, phenotype, and therapy. Horm Res Paediatr 75:81–89.

Binder G, Renz A, Martinez A, Keselman A, Hesse V, Riedl SW, Häusler G, Fricke-Otto S, Frisch H, Heinrich JJ, Ranke MB. 2004. SHOX haploinsufficiency and Leri–Weill dyschondrosteosis: Prevalence and growth failure in relation to mutation, sex, and degree of wrist deformity. J Clin Endocrinol Metab 89:4403–4408.

Chen J, Wildhardt G, Zhong Z, Röth R, Weiss B, Steinberger D, Decker J, Blum WF, Rappold G. 2009. Enhancer deletions of the SHOX gene as a frequent cause of short stature: The essential role of a 250 kb downstream regulatory domain. J Med Genet 46:834–839.

Clement-Jones M, Schiller S, Rao E, Blaschke RJ, Zuniga A, Zeller R, Robson SC, Binder G, Glass I, Strachan T, Lindsay S, Rappold GA. 2000. The short stature homeobox gene SHOX is involved in skeletal abnormalities in Turner syndrome. Hum Mol Genet 9:695–702.

Durand C, Bangs F, Signolet J, Decker E, Tickle C, Rappold G. 2010. Enhancer elements upstream of the SHOX gene are active in the developing limb. Eur J Hum Genet 18:527–532.

Fukami M, Okuyama T, Yamamori S, Nishimura G, Ogata T. 2005. Microdeletion in the SHOX 3′ region associated with skeletal phenotypes of Langer mesomelic dysplasia in a 45,X/46,X,r(X) infant and Leri–Weill dyschondrosteosis in her 46, XX mother: Implication for the SHOX enhancer. Am J Med Genet Part A 137A:72–76.

Fukami M, Kato F, Tajima T, Yokoya S, Ogata T. 2006. Transactivation function of an approximately 800-bp evolutionarily conserved sequence at the SHOX 3′ region: Implication for the downstream enhancer. Am J Hum Genet 78:167–170.

Fukami M, Dateki S, Kato F, Hasegawa Y, Mochizuki H, Horikawa R, Ogata T. 2008. Identification and characterization of cryptic SHOX intragenic deletions in three Japanese patients with Léri–Weill dyschondrosteosis. J Hum Genet 53:454–459.

Gordon CT, Tan TY, Benko S, Fitzpatrick D, Lyonnet S, Farlie PG. 2009. Long-range regulation at the SOX9 locus in development and disease. J Med Genet 46:649–656.

Mullen RD, Park S, Rhodes SJ. 2012. A distal modular enhancer complex acts to control pituitary- and nervous system-specific expression of the LHX3 regulatory gene. Mol Endocrinol 26:308–319.

Ogata T, Matsuo N, Nishimura G. 2001. SHOX haploinsufficiency and overdosage: Impact of gonadal function status. J Med Genet 38: 1–6.

Pennacchio LA, Ahituv N, Moses AM, Prabhakar S, Nobrega MA, Shoukry M, Minovitsky S, Dubchak I, Holt A, Lewis KD, Plajzer-Frick I, Akiyama J, De Val S, Afzal V, Black BL, Couronne O, Eisen MB, Visel A, Rubin EM. 2006. In vivo enhancer analysis of human conserved non-coding sequences. Nature 23:499–502.

Rao E, Weiss B, Fukami M, Rump A, Niesler B, Mertz A, Muroya K, Binder G, Kirsch S, Winkelmann M, Nordsiek G, Heinrich U, Breuning MH, Ranke MB, Rosenthal A, Ogata T, Rappold GA. 1997. Pseudoautosomal deletions encompassing a novel homeobox gene cause growth failure inidiopathic short stature and Turner syndrome. Nat Genet 16:54–63.

Rosilio M, Huber-Lequesne C, Sapin H, Carel JC, Blum WF, Cormier-Daire V. 2012. Genotypes and phenotypes of children with SHOX deficiency in France. J Clin Endocrinol Metab 97:E1257–E1265.

Sabherwal N, Bangs F, Röth R, Weiss B, Jants K, Tiecke E, Hinkel GK, Spaich C, Hauffa BP, van der Kamp H, Kapeller J, Tickle C, Rappold G. 2007. Long-range conserved non-coding SHOX sequences regulate expression in developing chicken limb and are associated with short stature phenotypes in human patients. Hum Mol Genet 16:210–222.

Shears DJ, Vassal HJ, Goodman FR, Palmer RW, Reardon W, Superti-Furga A, Scambler PJ, Winter RM. 1998. Mutation and deletion of the pseudoautosomal gene SHOX cause Leri–Weill dyschondrosteosis. Nat Genet 19:70–73.

Siracusa MC, Saenz SA, Hill DA, Kim BS, Headley MB, Doering TA, Wherry EJ, Jessup HK, Siegel LA, Kambayashi T, Dudek EC, Kubo M, Cianferoni A, Spergel JM, Ziegler SF, Comeau MR, Artis D. 2011. TSLP promotes interleukin-3-independent basophil haematopoiesis and type 2 inflammation. Nature 14:229–233.

Zinn AR, Wei F, Zhang L, Elder FF, Scott CI Jr, Marttila P, Ross JL. 2002. Complete SHOX deficiency causes Langer mesomelic dysplasia. Am J Med Genet 110:158–163.

Pediatr Transplantation 2014: 18: E25–E30



Pediatric Transplantation
DOI: 10.1111/petr.12184

# Selective expansion of donor-derived regulatory T cells after allogeneic bone marrow transplantation in a patient with IPEX syndrome

Horino S, Sasahara Y, Sato M, Niizuma H, Kumaki S, Abukawa D, Sato A, Imaizumi M, Kanegane H, Kamachi Y, Sasaki S, Terui K, Ito E, Kobayashi I, Ariga T, Tsuchiya S, Kure S. Selective expansion of donor-derived regulatory T cells after allogeneic bone marrow transplantation in a patient with IPEX syndrome.

Abstract: IPEX syndrome is a rare and fatal disorder caused by absence of regulatory T cells (Tregs) due to congenital mutations in the Forkhead box protein 3 gene. Here, we report a patient with IPEX syndrome treated with RIC followed by allogeneic BMT from an HLA-matched sibling donor. We could achieve engraftment and regimen-related toxicity was well tolerated. Although the patient was in mixed chimera and the ratio of donor cells in whole peripheral blood remained relatively low, selective and sustained expansion of Tregs determined as CD4+CD25+Foxp3+ cells was observed. Improvement in clinical symptoms was correlated with expansion of donor-derived Tregs and disappearance of anti-villin autoantibody, which was involved in the pathogenesis of gastrointestinal symptoms in IPEX syndrome. This clinical observation suggests that donor-derived Tregs have selective growth advantage in patients with IPEX syndrome even in mixed chimera after allogeneic BMT and contribute to the control of clinical symptoms caused by the defect of Tregs.

**Satoshi Horino[1,2], Yoji Sasahara[1], Miki Sato[1], Hidetaka Niizuma[1], Satoru Kumaki[1], Daiki Abukawa[3], Atsushi Sato[2], Masue Imaizumi[2], Hirokazu Kanegane[4], Yoshiro Kamachi[5], Shinya Sasaki[6], Kiminori Terui[6], Etsuro Ito[6], Ichiro Kobayashi[7], Tadashi Ariga[7], Shigeru Tsuchiya[1] and Shigeo Kure[1]**

[1]Department of Pediatrics, Tohoku University Graduate School of Medicine, Sendai, Miyagi, Japan, [2]Department of Hematology and Oncology, Miyagi Children's Hospital, Sendai, Miyagi, Japan, [3]Department of General Pediatrics, Miyagi Children's Hospital, Sendai, Miyagi, Japan, [4]Department of Pediatrics, Graduate School of Medicine and Pharmaceutical Science, University of Toyama, Toyama, Toyama, Japan, [5]Department of Pediatrics, Nagoya University Graduate School of Medicine, Nagoya, Aichi, Japan, [6]Department of Pediatrics, Hirosaki University School of Medicine, Hirosaki, Aomori, Japan, [7]Department of Pediatrics, Hokkaido University Graduate School of Medicine, Sapporo, Hokkaido, Japan

Key words: allogeneic hematopoietic stem cell transplantation – enteropathy – Forkhead box protein 3 – immune dysregulation – polyendocrinopathy – reduced intensity conditioning – regulatory T cells – X-linked syndrome

Yoji Sasahara, Department of Pediatrics, Tohoku University Graduate School of Medicine, 1-1 Seiryou-machi, Aoba-ku, Sendai, Miyagi 980-8574, Japan
Tel: +81 22 717 7287
Fax: +81 22 717 7290
E-mail: ysasahara@med.tohoku.ac.jp

Accepted for publication 24 September 2013

Abbreviations: ALL, acute lymphoblastic leukemia; APC, allophycocyanin; ATG, antithymocyte globulin; BMT, bone marrow transplantation; CyA, cyclosporine A; DAB, 3, 3′-diaminobenzidine; DLI, donor leukocyte infusion; FITC, fluorescein isothiocyanate; GST, glutathione-S-transferase; GVHD, graft-vs.-host disease; HLA, human leukocyte antigen; HSCT, hematopoietic stem cell transplantation; IPEX, immune dysregulation, polyendocrinopathy, enteropathy, X-linked; IVIG, intravenous immunoglobulin; MLL, mixed lineage leukemia; PBMCs, peripheral blood mononuclear cells; PBSCT, peripheral blood stem cell transplantation; PE, phycoerythrin; PSL, prednisolone; RIC, reduced intensity conditioning; TBI, total body irradiation.

IPEX syndrome is primary immunodeficiency caused by the defects of regulatory T cells (Tregs). IPEX syndrome is often lethal in the first few months of life due to severe diarrhea associated with refractory enteropathy, infections, diabetes mellitus, dermatitis, and other autoimmune complications. This disorder is caused by mutations of Forkhead box protein 3 (*FOXP3*) gene located on chromosome Xp11.23. *FOXP3* encodes Forkhead box protein 3, which is essential for the development and maintenance of CD4+CD25+Foxp3+ Tregs (1, 2).

Established treatments for patients with IPEX syndrome include immunosuppressive therapy and allogeneic HSCT (3–6). Allogeneic HSCT serves as a curative therapy for patients with IPEX syndrome, and RIC regimens have been reported and resulted in better outcome than myeloablative conditioning regimen (7–11). In general, allogeneic HSCT with RIC regimen may increase the risk of rejection and mixed chimera. Some RIC regimens included the antibody against T lymphocytes such as alemtuzumab or ATG. However, these agents may increase the risk of viral reactivation after HSCT. To the best of our knowledge, only two cases of IPEX patients treated with allogeneic HSCT following RIC consisted of low-dose TBI instead of alemtuzumab or ATG have been reported (12).

Here, we report a patient with IPEX syndrome treated with RIC regimen consisted of fludarabine, cyclophosphamide, and low-dose TBI followed by allogeneic HSCT from an HLA-identical sibling donor. Although the patient was in mixed chimera, he was free from symptoms caused by the absence of Tregs. We could observe selective and sustained growth advantage of donor-derived Tregs and disappearance of anti-villin autoantibody in his serum, which was correlated with the improvement in refractory enteropathy.

## Patient and methods

### Patient

A Japanese male suffered from severe diarrhea at two months of age. He was diagnosed as IPEX syndrome by identifying a missense mutation of T1117G substitution in exon 10 of the *FOXP3* gene (13). We quantified CD4+CD25+Foxp3+ cells by flow cytometry, and positive cells were not identified at all in PBMCs. Autoantibodies examined were negative except anti-villin antibody in patient's serum. He was treated with immunosuppressive therapy of intravenous CyA and oral PSL. After complete remission was achieved, he was free from the symptom for six yr with oral low-dose CyA and PSL (14).

At the age of six, the patient suffered from severe diarrhea again and was referred to our hospital. Although he was treated with increased doses of CyA and PSL in addition to other immunosuppressive agents, these treatments were not effective enough to control his diarrhea completely. We next tried IVIG therapy, which resulted in the improvement in diarrhea, and we could taper immunosuppressive agents.

To control the disease without continuous immunosuppressive therapy, we considered to perform allogeneic BMT from an HLA-matched healthy sibling donor. The donor did not have the mutation in *FOPX3* gene. We used a RIC regimen consisted of 4 Gy (2 × 2 Gy) TBI (day 7), fludarabine at a dose of 30 mg/m$^2$ for five days (days 6 to day 2) and cyclophosphamide at a dose of 60 mg/kg for two days (days 3 and 2). Total nucleated bone marrow cells of $4.32 \times 10^8$/kg were transplanted. We selected CyA and short-term methotrexate as GVHD prophylaxis, and IVIG was continued weekly until autoimmune colitis was resolved.

### Chimerism assay

Chimerism assay was performed by polymerase-chain-reaction-based assays analyzing polymorphic short tandem repeat markers (15). The chimerism was examined in each fraction of T cells, total lymphocytes, and granulocytes in bone marrow or peripheral blood. We evaluated the chimerism in bone marrow before day 100 and in peripheral blood after day 100, because we had similar results in both samples before day 100 in the patient and avoided frequent bone marrow aspiration after day 100.

### Flow cytometry

PBMCs were stained with monoclonal antibodies of APC-conjugated human CD4, PE-conjugated human CD25, and FITC-conjugated human Foxp3 antibodies (BD Biosciences, San Jose, CA, USA) and analyzed by a FACSCanto II flow cytometer (BD Biosciences), as described previously (16).

### Immunoblot analysis of anti-villin antibody

Anti-villin autoantibody in patient's serum was analyzed as described previously (17). Briefly, 500 ng of GST-villin recombinant protein (121 kD) was transferred to the membrane and incubated with diluted serum at 1:160. Anti-villin antibody bound to GST-villin was detected by horseradish peroxidase-conjugated antibody and DAB system.

## Case report

### Clinical improvement after RIC and allogeneic HSCT

The patient achieved an engraftment on day 11, and the last transfusion of platelets was on day 7 and that of red blood cells was on day 1. He was complicated with transient acute GVHD of the skin (grade I) on day 35 but this resolved without additional immunosuppressive therapy. He had no episodes of significant infection and other severe regimen-related toxicity during the course of RIC and allogeneic HSCT.

Severe and bloody diarrhea settled down on day 14 after engraftment. The patient was

consistently free from symptoms of enteropathy and any other autoimmune diseases. Laboratory findings showed improvement in hypoalbuminemia and anemia caused by severe enteropathy on day 21. Colonoscopy examination on day 60 revealed disappearance of mucosal inflammation, multiple ulcerations and hemorrhage that were observed before the HSCT.

After the discharge on day 120, we had followed the patient every two wk. He had no episodes of autoimmune disorders and infection, and we could taper and stop immunosuppressive agents at six months. Unfortunately, he suffered from MLL gene-rearranged ALL at 24 months after transplantation. The origin of precursor B lymphoblasts was recipient cells. We treated him with chemotherapy and allogeneic PBSCT from the same donor. We used myeloablative conditioning regimen consisted of busulfan at a dose of 4 mg/kg for four days and melphalan at a dose of 90 mg/m$^2$ for two days for the second transplant from the same sibling donor to cure this secondary ALL. He has been in complete remission for more than two yr. Chimerism completely changed to donor-type and the number of Tregs increased to normal after the second transplant.

### Chimerism and immunological evaluation after first allogeneic HSCT

Because the ratio of donor T cells, total lymphocytes, and granulocytes in bone marrow was 74%, 48%, and 48%, respectively, on day 22 after HSCT, we reduced the dose of CyA immediately. The ratio of donor cells, however, was further declined to 5% on day 50, and the donor bone marrow was assumed to be rejected (Fig. 1). At that point, flow cytometric analysis of peripheral blood showed that 17.8% of PBMCs were CD4+CD25+Foxp3+ Tregs (Fig. 2a,b). This discordant result on day 50 was explained by selective expansion of donor-derived Tregs. After discontinuation of CyA on day 50, the ratio of donor T cells, total lymphocytes, and granulocytes was transiently increased up to 40% and then gradually decreased (Fig. 1). At 24 months after HSCT, donor cells were around 20% and CD4+CD25+Foxp3+ Tregs were at the range of 1.2–3.0% of PBMCs, which were comparable to healthy controls (Fig. 2a). We did not perform DLI because the ratio of donor cells was <50% and supposed that the patient was in high risk of bone marrow aplasia after repeated DLI.

The anti-villin autoantibody was detected by immunoblot analysis when the disease was active before HSCT. The antibody was under detectable levels both in clinical remission by immunosuppressive therapy before HSCT and after engraftment was achieved following HSCT even when immunosuppressive agents were not administrated (Table 1).

## Discussion

The defect of Tregs in patients with IPEX syndrome causes symptoms related to

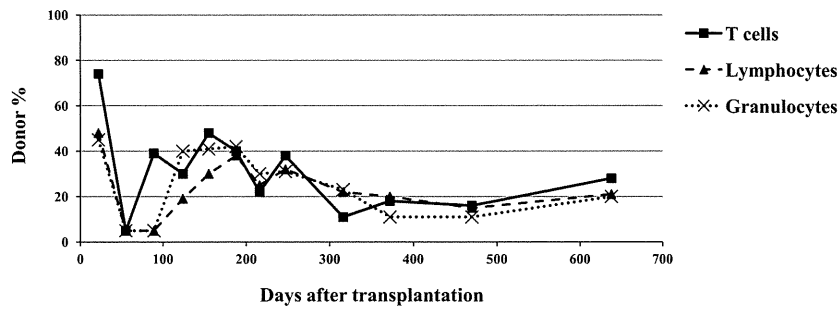


*Fig. 1.* Frequency of donor cells after allogeneic HSCT. Percentages of donor cells in each fraction of T cells, total lymphocytes, and granulocytes after HSCT are shown.

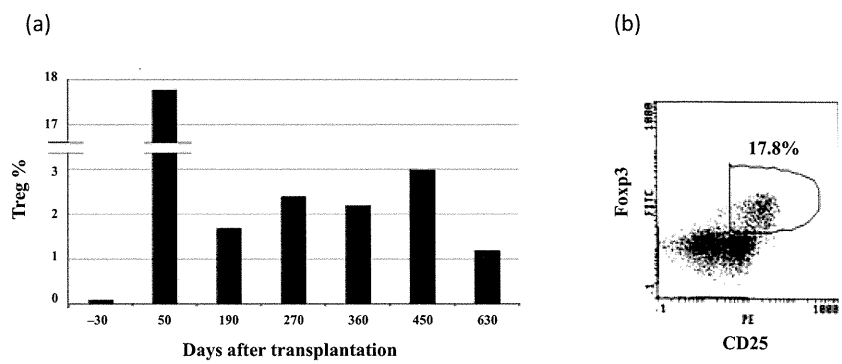


*Fig. 2.* Sustained expansion of donor Tregs after allogeneic HSCT. (a) Percentages of Tregs are evaluated as CD4+CD25+Foxp3+ cells in PBMCs. (b) Flow cytometric demonstration of CD25+Foxp3+ cells in CD4 gated PBMCs on day 50 after HSCT.

Table 1. Anti-villin autoantibody is correlated with clinical condition of enteropathy

| Clinical condition of enteropathy | Anti-villin autoantibody |
|---|---|
| Disease onset | + |
| Remission before HSCT | − |
| Relapse before HSCT | + |
| After HSCT | − |

GST-villin protein (121 kD) was transferred to the membrane, and immunoblot was performed with 1:160 diluted patient's serum at different disease condition of enteropathy as indicated. + indicates the presence of anti-villin antibody that recognizes GST-villin protein.

autoimmunity. However, clinical benefit of immunosuppressive therapy is often limited by its adverse effects and increased susceptibility to infection. At present, allogeneic HSCT is recognized as the curative therapy for patients with IPEX syndrome. We summarized all reported cases treated with HSCT in Table 2. Myeloablative regimen resulted in high fatality due to regimen-related toxicity or lethal infection (2, 5, 6). On the other hand, Rao et al. (7) first reported four patients who were successfully treated with non-myeloablative conditioning regimen consisted of fludarabine, melphalan, and alemtuzumab, and achieved high rate of donor chimerism above 84.6%. Non-myeloablative regimens with anti-T-lymphocyte antibody such as alemtuzumab or ATG have been used, and all patients are alive (7–11). However, it is known that alemtuzumab and ATG induce profound depletion of T cells and increase the risk of viral reactivation and fungal infection after HSCT. Therefore, we used low-dose TBI instead of anti-T-lymphocyte antibodies. The combination of low-dose TBI, fludarabine, and cyclophosphamide was well tolerated, and the patient was free from infections and severe regimen-related toxicities. Burroughs et al. (12) also reported that RIC regimen including low-dose TBI for IPEX syndrome resulted in stable engraftment of Tregs and better clinical outcome, proposing that this regimen was preferable for patients with IPEX syndrome.

The patient developed MLL-related secondary ALL in recipient cells. Although the dose of TBI was less than used in myeloablative conditioning, radiation and alkylating agents might cause DNA damage and increased the risk of secondary leukemia in recipient cells. Alternatively, the use of anti-T-lymphocyte antibody instead of low-dose TBI and/or dose reduction in alkylating agents should be carefully considered in IPEX syndrome.

Selected and sustained expansion of Tregs resulted in clinical improvement even though the patient was in mixed chimera after HSCT. Seidel et al. (11) reported a patient with IPEX

Table 2. Summary of IPEX patients treated with allogeneic HSCT reported in the literature

| Case | Age | Donor | Conditioning regimen | Complications after HSCT | Outcome | % Donor after HSCT | Reference |
|---|---|---|---|---|---|---|---|
| 1 | 13 yr | HLA-matched sibling | TBI 12 Gy + CY + ATG | Adenovirus infection, pneumonia | Dead | 50% | 2 |
| 2 | 9 yr | HLA-matched unrelated | TBI 12 Gy + CY + ATG | Cytomegalovirus infection, hemorrhagic cystitis, lymphoproliferative disorder | Dead | 70% | 2 |
| 3 | 4 months | HLA-matched sibling | BU + CY + ALG | Hemophagocytic syndrome | Dead | 30% in T cell | 5 |
| 4 | 1 yr | HLA-matched sibling | BU + CY + Flu + ATG | | Alive | 70% in T cell | 6 |
| 5 | 7 yr | HLA-matched unrelated | Flu + L-PAM + alemtuzumab | Cytomegalovirus infection | Alive | 100% | 7 |
| 6 | 1 yr | HLA-matched unrelated | Flu + L-PAM + alemtuzumab | Acute respiratory distress syndrome | Alive | 100% | 7 |
| 7 | 4 yr | HLA-matched sibling | Flu + L-PAM + alemtuzumab | Histoplasma infection | Alive | 89% | 7 |
| 8 | 5 months | HLA-matched unrelated | Flu + L-PAM + alemtuzumab | | Alive | 84.6% | 7 |
| 9 | 7 yr | HLA 5/6-matched cord blood | Flu + BU + ATG | Lymphoproliferative disorder | Alive | 81 ~ 98% | 8 |
| 10 | 7 months | HLA-matched unrelated | Flu + L-PAM + alemtuzumab | Sepsis of *Enterobacter cloacae* | Alive | 100% | 9 |
| 11 | 5 months | HLA-matched unrelated | Flu + L-PAM + alemtuzumab + anti-CD 45 monoclonal antibody | | Alive | 100% | 10 |
| 12 | 11 months | HLA-matched unrelated | Flu + L-PAM + alemtuzumab | | Alive | <10% | 11 |
| 13 | 9 months | HLA-matched unrelated | TBI 4 Gy + Flu | Bacteremia | Alive | 100% | 12 |
| 14 | 16 yr | HLA-matched related | TBI 4 Gy + Flu | Bacteremia | Alive | 20 ~ 60% in T cell | 12 |

Case series transplanted with RIC regimens were highlighted.
CY, cyclophosphamide; ALG, antilymphocyte globulin; BU, busulfan; Flu, fludarabine; L-PAM, melphalan.

syndrome who showed selective engraftment of Tregs for six yr after non-myeloablative transplantation. It has been reported that partial BMT or injection of T-enriched splenocytes resulted in the rescue of autoimmunity in Scurfy mice, a mouse model for IPEX syndrome in which *FOXP3* gene is naturally mutated. Sustained engraftment of relatively high frequency of CD4+CD25+Foxp3+ Tregs was observed even though the frequency of donor cells in whole peripheral blood ranged from 1.7% to 50% (18). These observations illustrate that the paradigm in the generation of Tregs is reinforced by the requirement and growth advantage regardless of chimerism of other hematopoietic cells in IPEX syndrome. However, we should still consider the possibility that mixed chimerism may result in subsequent development of autoimmune diseases observed in other primary immunodeficiency, as previously reported in some patients with Wiskott–Aldrich syndrome (19).

Intractable diarrhea is a major symptom in patients with IPEX syndrome. Villin, an actin-binding protein, is expressed as the 95 kD antigen in the small intestine, which is frequently targeted by autoantibodies in patients with IPEX syndrome (17). Anti-villin antibody was clearly correlated with the severity of clinical symptoms in our patient. Therefore, monitoring of anti-villin antibody might serve as a useful examination for evaluating gastrointestinal complications in patients with IPEX syndrome.

We reported here a unique phenomenon of selective growth advantage of Tregs in a patient with IPEX syndrome who was in mixed chimera after RIC and allogeneic HSCT. Sustained expansion of donor-derived Tregs resulted in the significant improvement in enteropathy. To determine optimal RIC regimen to achieve complete chimera and avoid secondary malignancy in residual recipient cells, further analysis in more patients and long-term follow-up study after HSCT are required to conclude this issue.

### Authors' contributions

Horino S and Sasahara Y designed the study, interpreted the data, wrote the paper, and treated the patient. Sato M, Kanegane H, Kamachi Y, and Kobayashi I performed experiments. All other authors treated the patient and collected clinical data.

### Acknowledgments

We thank all of our colleagues in the Department of Pediatrics, Tohoku University, who contributed to the patient's care. This work was supported by the grants-in-aid from the Ministry of Education, Culture, Sports, Science, and Technology of Japan (23591528 to YS), a grant for research on intractable diseases from the Ministry of Health, Labour and Welfare of Japan (to YS), grants from Japan Leukemia Research Fund and SENSHIN Medical Research Foundation (to YS).

### Conflict of interest disclosure

The authors declare no conflict of interest.

## References

1. Powell BR, Bruist NR, Stenzel P. An X-linked syndrome of diarrhea, polyendocrinopathy, and fatal infection in infancy. J Pediatr 1982: 100: 731–737.
2. Wildin RS, Smyk-Pearson S, Filipovich AH. Clinical and molecular features of the immunodysregulation, polyendocrinopathy, enteropathy, X-linked (IPEX) syndrome. J Med Genet 2002: 39: 537–545.
3. Taddio A, Faleschini E, Valencic E, et al. Medium-term survival without hematopoietic stem cell transplantation in a case of IPEX: Insights into nutritional and immunosuppressive therapy. Eur J Pediatr 2007: 166: 1195–1197.
4. Gambineri E, Perroni L, Passerini L, et al. Clinical and molecular profile of a new series of patients with immune dysregulation, polyendocrinopathy, enteropathy, X-linked syndrome: Inconsistent correlation between forkhead box protein 3 expression and disease severity. J Allergy Clin Immunol 2008: 122: 1105–1112.
5. Baud O, Goulet O, Canioni D, et al. Treatment of the immune dysregulation, polyendocrinopathy, enteropathy, X-linked syndrome (IPEX) by allogeneic bone marrow transplantation. N Engl J Med 2001: 344: 1758–1762.
6. Mazzolari E, Forino C, Fontana M, et al. A new case of IPEX receiving bone marrow transplantation. Bone Marrow Transplant 2005: 35: 1033–1034.
7. Rao A, Kamani N, Filopovich A, et al. Successful bone marrow transplantation for IPEX syndrome after reduced-intensity conditioning. Blood 2007: 109: 383–385.
8. Lucas KG, Ungar D, Comito M, et al. Submyeloablative cord blood transplantation corrects clinical defects seen in IPEX syndrome. Bone Marrow Transplant 2007: 39: 55–56.
9. Dorsey MJ, Petrovic A, Morrow MR, et al. FOXP3 expression following bone marrow transplantation for IPEX syndrome after reduced-intensity conditioning. Immunol Res 2009: 44: 179–184.
10. Zhan H, Sinclair J, Adams S, et al. Immune reconstitution and recovery of FOXP3 (forkhead box protein 3)-expressing T cells after transplantation for IPEX (immune dysregulation, polyendocrinopathy, enteropathy, X-linked) syndrome. Pediatrics 2008: 121: 998–1002.
11. Seidel MG, Fritsch G, Lion T, et al. Selective engraftment of donor $CD4^{+}CD25^{high}$ FOXP3-positive T cells in IPEX syndrome after nonmyeloablative hematopoietic stem cell transplantation. Blood 2009: 113: 5689–5691.
12. Burroughs LM, Torgerson TR, Storb R, et al. Stable hematopoietic cell engraftment after low-intensity nonmyeloablative conditioning in patients with immune dysregulation, polyendocrinopathy, enteropathy, X-linked syndrome. J Allergy Clin Immunol 2010: 126: 1000–1005.
13. Tanaka H, Suzuki K, Nakahata T, et al. Immune dysregulation, polyendocrinopathy, enteropathy, X-linked syndrome. Acta Paediatr 2004: 93: 142–143.
14. Tanaka H, Tsugawa K, Kudo M, et al. Low-dose cyclosporine A in a patient with X-linked immune dysregulation, polyendocrinopathy and enteropathy. Eur J Pediatr 2005: 164: 779–780.

15. Thiede C, Florek M, Bornhäuser M, et al. Rapid quantification of mixed chimerism using multiplex amplification of short tandem repeat markers and fluorescence detection. Bone Marrow Transplant 1999: 23: 1055–1060.
16. Otsubo K, Kanegane H, Kamachi Y, et al. Identification of FOXP3-negative regulatory T-like ($CD4^+CD25^+CD127^{low}$) cells in patients with immune dysregulation, polyendocrinopathy, enteropathy, X-linked syndrome. Clin Immunol 2011: 141: 111–120.
17. Kobayashi I, Kubota M, Yamada M, et al. Autoantibodies to villin occur frequently in IPEX, a severe immune dysregulation, syndrome caused by mutation of FOXP3. Clin Immunol 2011: 141: 83–89.
18. Smyk-Pearson SK, Bakke AC, Held PK, et al. Rescue of the autoimmune scurfy mouse by partial bone marrow transplantation or injection with T-enriched splenocytes. Clin Exp Immunol 2003: 133: 193–199.
19. Ozsahin H, Cavazzana-Calvo M, Notarangelo LD, et al. Long-term outcome following hematopoietic stem-cell transplantation in Wiskott-Aldrich syndrome: Collaborative study of the European Society for Immunodeficiencies and European Group for Blood and Marrow Transplantation. Blood 2008: 111: 439–445.

*Human Molecular Genetics, 2014, Vol. 23, No. 4* **992–1001**
*doi:10.1093/hmg/ddt495*
*Advance Access published on October 8, 2013*

# RNA sequencing-based identification of aberrant imprinting in cloned mice

**Hiroaki Okae[1,3,†], Shogo Matoba[4,†], Takeshi Nagashima[2], Eiji Mizutani[4,5], Kimiko Inoue[4], Narumi Ogonuki[4], Hatsune Chiba[1,3], Ryo Funayama[2], Satoshi Tanaka[6], Nobuo Yaegashi[7], Keiko Nakayama[2], Hiroyuki Sasaki[3,8], Atsuo Ogura[4] and Takahiro Arima[1,3,*]**

[1]Department of Informative Genetics, Environment and Genome Research Center, [2]Division of Cell Proliferation, United Centers for Advanced Research and Translational Medicine, Tohoku University Graduate School of Medicine, Sendai 980-8575, Japan [3]JST, CREST, Saitama 332-0012, Japan [4]RIKEN BioResource Center, Tsukuba, Ibaraki 305-0074, Japan [5]Faculty of Life and Environmental Sciences, University of Yamanashi, Kofu 400-8510, Japan [6]Laboratory of Cellular Biochemistry, Department of Animal Resource Sciences/Veterinary Medical Sciences, The University of Tokyo, Tokyo 113-8657, Japan [7]Department of Obstetrics and Gynecology, Tohoku University Graduate School of Medicine, Sendai 980-8574, Japan and [8]Division of Epigenomics, Department of Molecular Genetics, Medical Institute of Bioregulation, Kyushu University, Fukuoka 812-8582, Japan

Received May 8, 2013; Revised August 19, 2013; Accepted October 2, 2013

**Animals cloned by somatic cell nuclear transfer (SCNT) provide a unique model for understanding the mechanisms of nuclear epigenetic reprograming to a state of totipotency. Though many phenotypic abnormalities have been demonstrated in cloned animals, the underlying mechanisms are not well understood. In this study, we performed transcriptome-wide allelic expression analyses in brain and placental tissues of cloned mice. We found that *Gab1*, *Sfmbt2* and *Slc38a4* showed loss of imprinting in all cloned mice analyzed, which might be involved in placentomegaly of cloned mice. These three genes did not require *de novo* DNA methylation in growing oocytes for the establishment of imprinting, implying the involvement of a *de novo* DNA methylation-independent mechanism. Loss of *Dlk1-Dio3* imprinting was also observed in nearly half of cloned mouse embryos and showed a strong correlation with embryonic lethality. Our findings are essential to understand the underlying mechanisms of developmental abnormalities of cloned animals. We also emphasize that particular attention should be paid to specific imprinted genes for therapeutic and agricultural applications of SCNT.**

## INTRODUCTION

Animals cloned by somatic cell nuclear transfer (SCNT) provide a unique model for understanding the mechanisms of nuclear epigenetic reprograming to a state of totipotency (1,2). However, the cloning efficiency is very low regardless of the animal species or donor cell type. Though many phenotypic abnormalities have been demonstrated in cloned animals, including frequent embryonic and perinatal death and placentomegaly, the underlying mechanisms are not well understood (3).

Genomic imprinting is an epigenetic gene regulatory mechanism that leads to the preferential expression of the paternally or maternally inherited allele of a subset of genes. Most notably, DNA methylation, which occurs at discrete locations termed differentially methylated regions (DMRs) in the germline, initiates the imprinting process (4). The *de novo* methyltransferase Dnmt3a and the Dnmt3-related protein Dnmt3L are required for the establishment of germline DMRs (5,6). The majority of imprinted genes reside within imprinted domains, and these DMRs are known to control imprinted gene expression within the domain (7). Abnormal expression of some imprinted genes causes developmental defects (8), some of which are similar to those observed in cloned animals.

*To whom correspondence should be addressed at: Department of Informative Genetics, Environment and Genome Research Center, Tohoku University Graduate School of Medicine, 2-1 Seiryo-machi, Aoba-ku, Sendai 980-8575, Japan. Tel: 81 227177844; Fax:+ 81 227177063; Email: tarima@med.tohoku.ac.jp
†H.O. and S.M. contributed equally to this work.

Abnormal imprinting of some imprinted genes has been reported in cloned animals (9–11). In particular, abnormal allelic expression or DMR methylation of *H19*, *Igf2r*, *Peg3*, *Snrpn*, *Ascl2* and *Xist* has been reported in cloned mice (12–16). However, the vast majority of the abnormalities are only partial loss of imprinting or donor cell type-specific. For example, aberrant imprinting of *H19* and *Igf2* was frequently observed in embryonic stem cell-derived cloned mice (14), but not in somatic cell-derived ones (17). Furthermore, the relationships between developmental defects and imprinting abnormalities are poorly understood in cloned mice. The only exception is ectopic expression of *Xist*, which occurs in nearly all cloned mouse embryos, and accounts for embryonic loss at the postimplantation stage (16,18). Importantly, Inoue *et al.* reported faithful monoallelic expression of seven well-known imprinted genes in cloned mouse embryos (17). Overall, the memory of genomic imprinting is believed to be stably maintained in cloned mice with the exception of *Xist*.

In the mouse, ~100 imprinted genes have been identified, but the imprinting status of most known imprinted genes has not been analyzed in cloned mice. Especially, we recently reported placenta-specific imprinted genes, which show imprinted expression in the placenta but are biallelically expressed in the fetus (19). It is possible that the nuclei of fetus-derived somatic cells do not acquire placenta-specific imprinting after SCNT. Therefore, we performed transcriptome-wide allelic expression analyses and found that three imprinted genes, including two placenta-specific imprinted genes, consistently showed loss of imprinting in all cloned mice analyzed (consistent loss of imprinting). We also verified the correlation between loss of *Dlk1-Dio3* imprinting and embryonic lethality of cloned mice.

## RESULTS

### Transcriptome-wide analyses of imprinted gene expression in cloned mouse placentas and brains

For whole transcriptome sequencing analyses, we selected the placenta and brain because many imprinted genes, including genes with tissue-specific imprinted expression, are known to be expressed in these tissues (19,20). 129X1/SvJ (129) females were mated with Japanese fancy 1 (JF1) males to generate [129xJF1]F1 mice from which cumulus and Sertoli cells were isolated and used for SCNT. F1 embryos were also generated by *in vitro* fertilization (IVF) to provide a comparison. Placentas and brains were dissected from embryonic day (E) 13.5 embryos and analyzed. Forty-five known imprinted genes had at least one single nucleotide polymorphism (SNP) site between 129 and JF1 and were expressed at a sufficient level to assess allelic expression in the placenta and/or brain (Supplementary Material, Table S1). For the analyses of allelic expression, the maternal read number divided by the paternal read number (M/P ratio) was calculated for each imprinted gene. The maternal expression and paternal expression are defined as [M/P ratio] >2 and [M/P ratio] <0.5, respectively. There were 28 and 25 genes that showed imprinted expression in all IVF-derived placentas and brains, respectively (Fig. 1). Of these, eight genes showed abnormal allelic expression in at least two cloned placentas or brains (boxed in Fig. 1, note that *Dlk1* showed aberrant expression in both tissues). Importantly, *Gab1*, *Sfmbt2* and *Slc38a4* showed biallelic expression in all cloned placentas analyzed (Fig. 1).

### Imprinting status of placenta-specific imprinted genes in cloned mouse placentas

Two paternally expressed placenta-specific imprinted genes, *Gab1* and *Sfmbt2*, were expressed biallelically in all cloned mouse placentas (Fig. 1). *Gab1* is mainly expressed via a placenta-specific promoter in the normal placenta and has a novel DMR that is acquired after implantation (Fig 2A and Supplementary Material, Fig. S1). *Gab1* was not detected in cumulus cells and showed biallelic expression in Sertoli cells (Fig. 2B). *Gab1* showed biallelic expression in all cloned placentas analyzed (Fig. 2B) and was expressed at a level twice as high as in the IVF-derived placentas (Fig. 2C). Maternal allele-specific methylation was lost in the cloned mouse placentas (Fig. 2D).

*Sfmbt2* was also biallelically expressed in the cloned mouse placentas, and the expression level was twice as high as that of the IVF-derived placentas (Fig. 2E and F). Though there is no direct DNA methylation of the *Sfmbt2* promoter region, we previously reported the enrichment of H3K9me2 and H3K27me3 on the maternal allele (19). This allele-specific accumulation of H3K9me2 and H3K27me3 was not observed in the cumulus-derived cloned mouse placenta and cumulus cells (Fig. 2G).

Unlike *Gab1* and *Sfmbt2*, other placenta-specific imprinted genes (*Ppp1r9a*, *Ascl2*, *Tssc4* and *Slc22a3*) showed normal maternal allele-specific expression in the cloned mouse placentas (Supplementary Material, Fig. S2A). Brain-specific imprinted genes also showed normal allelic expression in the cloned mouse brains (*Blcap* in Fig. 1; *Grb10* and *Ube3a* in Supplementary Material, Fig. S2B).

### Consistent loss of *Slc38a4* imprinting in cloned mice

*Slc38a4* shows paternal allele-specific expression both in embryonic and extraembryonic tissues and has a germline DMR (21,22). *Slc38a4* also showed paternal expression in donor cells but was biallelically expressed in the cloned mouse brains and placentas (Fig. 3A). Increased expression of *Slc38a4* was observed both in the cloned mouse brains and, to a lesser extent, in placentas (Fig. 3B). Maternal allele-specific methylation of the *Slc38a4* DMR was observed in cumulus cells but not in the cumulus-derived cloned mouse brain (Fig. 3C). Demethylation of the *Slc38a4* DMR was already evident in the cloned blastocysts (Fig. 3D) and also observed in adult cloned mice (Supplementary Material, Fig. S3A). Interestingly, the paternally biased expression was not lost in embryos obtained from *Dnmt3L*-deficient and oocyte-specific *Dnmt3a/3b*-deficient female mice (Fig. 3E). It is already reported that the *Slc38a4* DMR is not methylated at all in *Dnmt3L*-deficient oocytes (23). These data strongly suggested that during oocyte growth, *de novo* DNA methylation was dispensable for imprinted expression of *Slc38a4*.

### Correlation between loss of *Dlk1-Dio3* imprinting and embryonic lethality of cloned mice

Five imprinted genes showed abnormal allelic expression in some cloned placentas or brains (Fig. 1). Among them, we focused on *Dlk1* because the *Dlk1-Dio3* domain (Fig. 4A) is important for normal mouse development (24). *Dlk1* showed normal paternal expression in the donor cells (Fig. 4B). Biallelic expression of *Dlk1* was observed in the placentas and fetuses

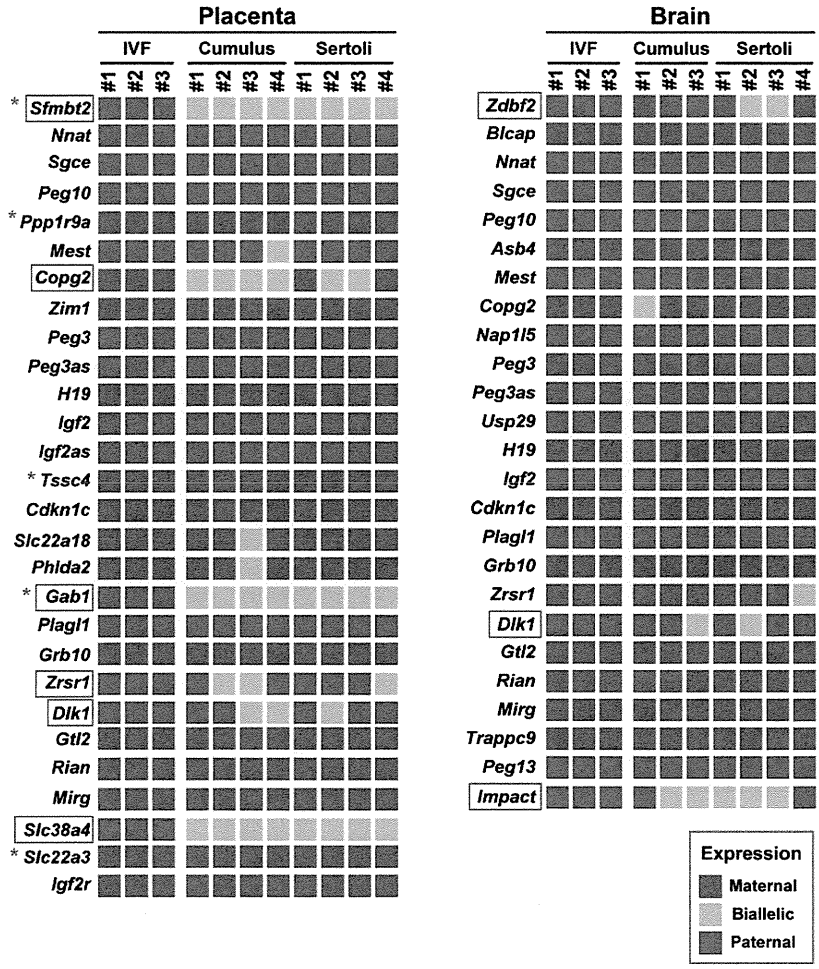


**Figure 1.** Transcriptome-wide analyses of imprinted gene expression in cloned mouse placentas and brains. The maternal read number divided by the paternal read number (M/P ratio) is color-coded. The maternal expression (red) and paternal expression (blue) are defined as [M/P ratio] $>2$ and [M/P ratio] $<0.5$, respectively. The biallelic expression (green) is defined as $2\geq$ [M/P ratio] $\geq 0.5$. Imprinted genes that showed abnormal allelic expression in at least two cloned placentas or brains are indicated by red boxes. Placenta-specific imprinted genes are marked with asterisks.

derived from cumulus clones #3 and #4 and Sertoli clone #2 (Fig. 4B and Supplementary Material, Fig. S4A). In the brains derived from cumulus clone #3 and Sertoli clone #2, *Dlk1* also showed biallelic expression (Fig. 4B). In the cloned mouse brains, biallelic expression of *Dlk1* correlated with increased expression of *Dlk1* (Fig. 4C). In the brains derived from cumulus clone #3 and Sertoli clone #2, biallelic expression of *Begain* and *Rtl1* (Supplementary Material, Fig. S4B) and downregulation of *Gtl2*, *Rian* and *Mirg* (Fig. 4C) were observed. Abnormal allelic expression of *Gtl2* was not observed in the cloned mouse brains (Supplementary Material, Fig. S4B).

In the cloned mouse placentas, the expression level of genes in the *Dlk1-Dio3* domain was extremely low regardless of allelic expression of *Dlk1* (Supplementary Material, Fig. S4C). In the placenta, *Dlk1* and *Gtl2* are mainly expressed in the labyrinth layer (25,26). The junctional zone, where *Dlk1* and *Gtl2* are not (or weakly) expressed, is expanded in the cloned mouse placenta (25). Therefore, low expression of *Dlk1* and *Gtl2* may, in part, be explained by the expansion of the junctional zone (relative reduction of the labyrinth layer) in the cloned mouse placenta.

Imprinting of the *Dlk1-Dio3* domain is regulated by the IG-DMR (24). Paternal methylation of the IG-DMR was observed in both the donor cells and the IVF-derived brain (Supplementary Material, Fig. S4D), but in the brains derived from cumulus clone #3 and Sertoli clone #2, both alleles were methylated (Fig. 4D). In the whole fetus of cumulus clone #4, gain of maternal methylation of the IG-DMR was also observed (Fig. 4D). Gain of maternal methylation of the IG-DMR was also found in the cloned placentas (Supplementary Material, Fig. S4E). Similar data were obtained for the *Gtl2*-DMR (Supplementary Material, Fig. S5).

Placental development without a viable fetus is frequently observed in SCNT (27). We compared the imprinting status of the *Dlk1-Dio3* domain in term placentas with and without viable fetuses, which were produced by a series of experiments using *Xist*-siRNA (Supplementary Material, Table S2). The use

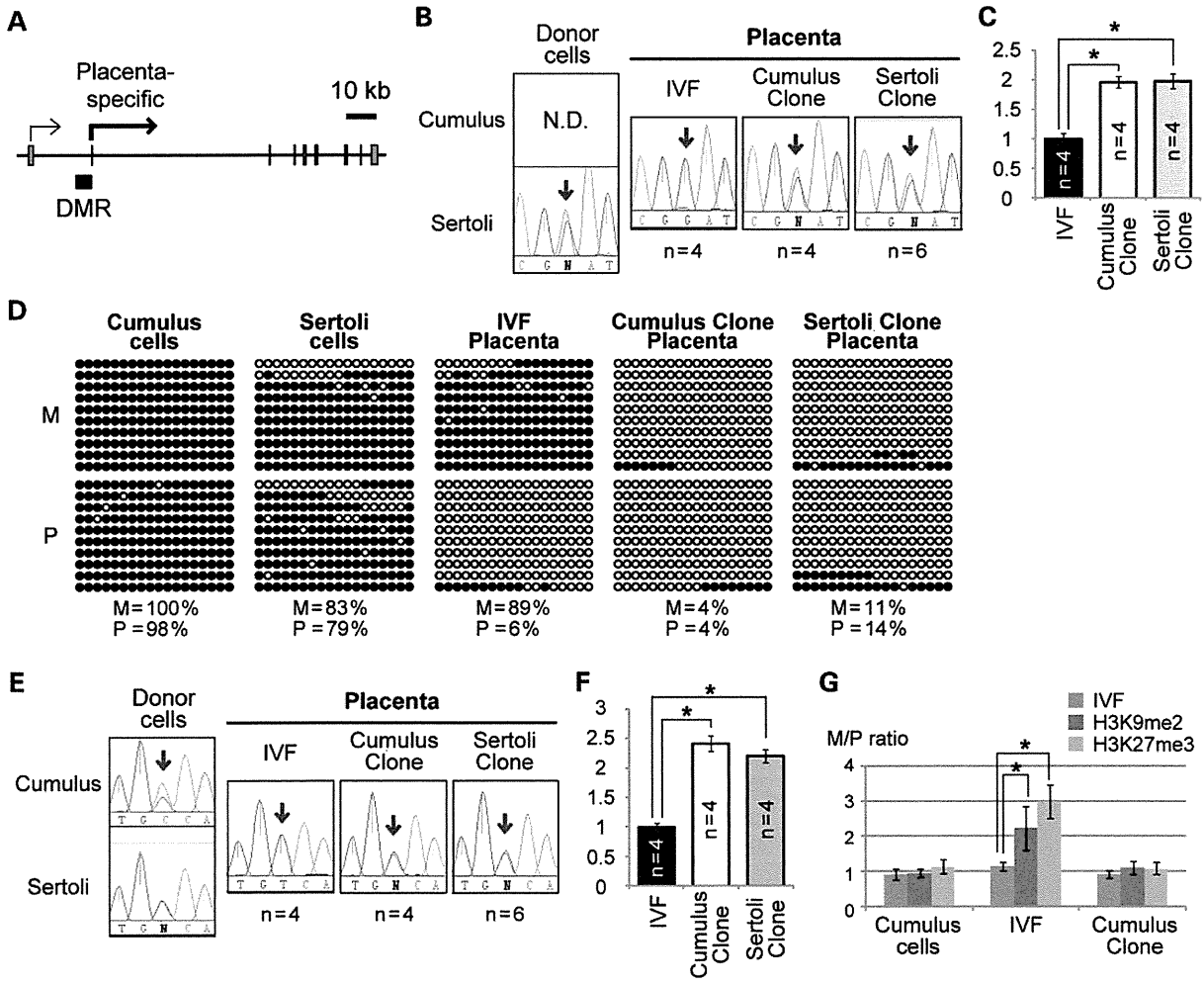


**Figure 2.** Consistent loss of *Gab1* and *Sfmbt2* imprinting in cloned mouse placentas. (**A**) Genomic structure of *Gab1*. The *Gab1* DMR and two transcription start sites are shown. Expression from the placenta-specific promoter was analyzed in this study. (**B**) Allelic expression of *Gab1*. *Gab1* showed paternal expression in all IVF-derived placentas but showed biallelic expression in all cloned mouse placentas. The numbers of analyzed samples are shown. Very similar data were obtained for all cloned placentas. The SNP site between 129 and JF1 is indicated by arrows. N.D.: not detected. (**C**) Real-time RT–PCR analysis of *Gab1*. The mean expression level of the IVF-derived placentas is set as 1. The error bars indicate means ± SD of four placentas. $^*P < 0.001$ (Student's *t*-test). (**D**) DNA methylation analysis of the *Gab1* DMR by bisulfite sequencing. Black and white circles indicate methylated and unmethylated residues, respectively. The percentages of methylated CpG sites of the maternal allele (M) and the paternal allele (P) are indicated. (**E**) Allelic expression of *Sfmbt2*. *Sfmbt2* showed paternal expression in all IVF-derived placentas but showed biallelic expression in all cloned mouse placentas. The numbers of analyzed samples are shown. Very similar data were obtained for all cloned placentas. (**F**) Real-time RT–PCR analysis of *Sfmbt2*. The error bars indicate means ± SD of four placentas. $^*P < 0.001$ (Student's *t*-test). (**G**) Histone modifications at *Sfmbt2* promoter region by chromatin immunoprecipitation (ChIP) and single nucleotide primer extension (SNuPE). The amount of immunoprecipitated DNA derived from the maternal allele is divided by that from the paternal allele (M/P ratio). The error bars indicate means ± SD from three samples. $^*P < 0.05$ (Student's *t*-test).

of *Xist*-siRNA increases cloning efficiency (18) and enables the comparison of placentas with and without viable fetuses within the same experiment. Biallelic expression of *Dlk1* was consistently observed in placentas, brains and fetuses (Fig. 4B and Supplementary Material, Fig. S4A). Therefore, if *Dlk1* shows biallelic expression in the placenta, it is predicted that *Dlk1* would also show biallelic expression in the brain and fetus. A clear increase of abnormal maternal expression of *Dlk1* was observed in the placentas without viable fetuses compared with the placentas with viable fetuses ($P < 10^{-9}$) (Fig. 4E), alongside hypermethylation of the IG-DMR (Supplementary Material, Fig. S6). On the other hand, allelic expression profiles of *Sgce* and *Zim1* were comparable between placentas with viable fetuses and without viable fetuses ($P > 0.05$, Supplementary Material, Fig. S4F).

### Confirmation of loss of imprinting in cloned mouse placentas produced without trichostatin A (TSA) treatment

Figures 1–4 present data from cloned mouse embryos produced using TSA to increase cloning efficiency. TSA treatment might affect allelic expression of some imprinted genes. Therefore, we confirmed biallelic expression of *Gab1*, *Sfmbt2* and *Slc38a4* in four cloned mouse placentas produced without TSA treatment (Supplementary Material, Fig. S3B). Similarly, biallelic

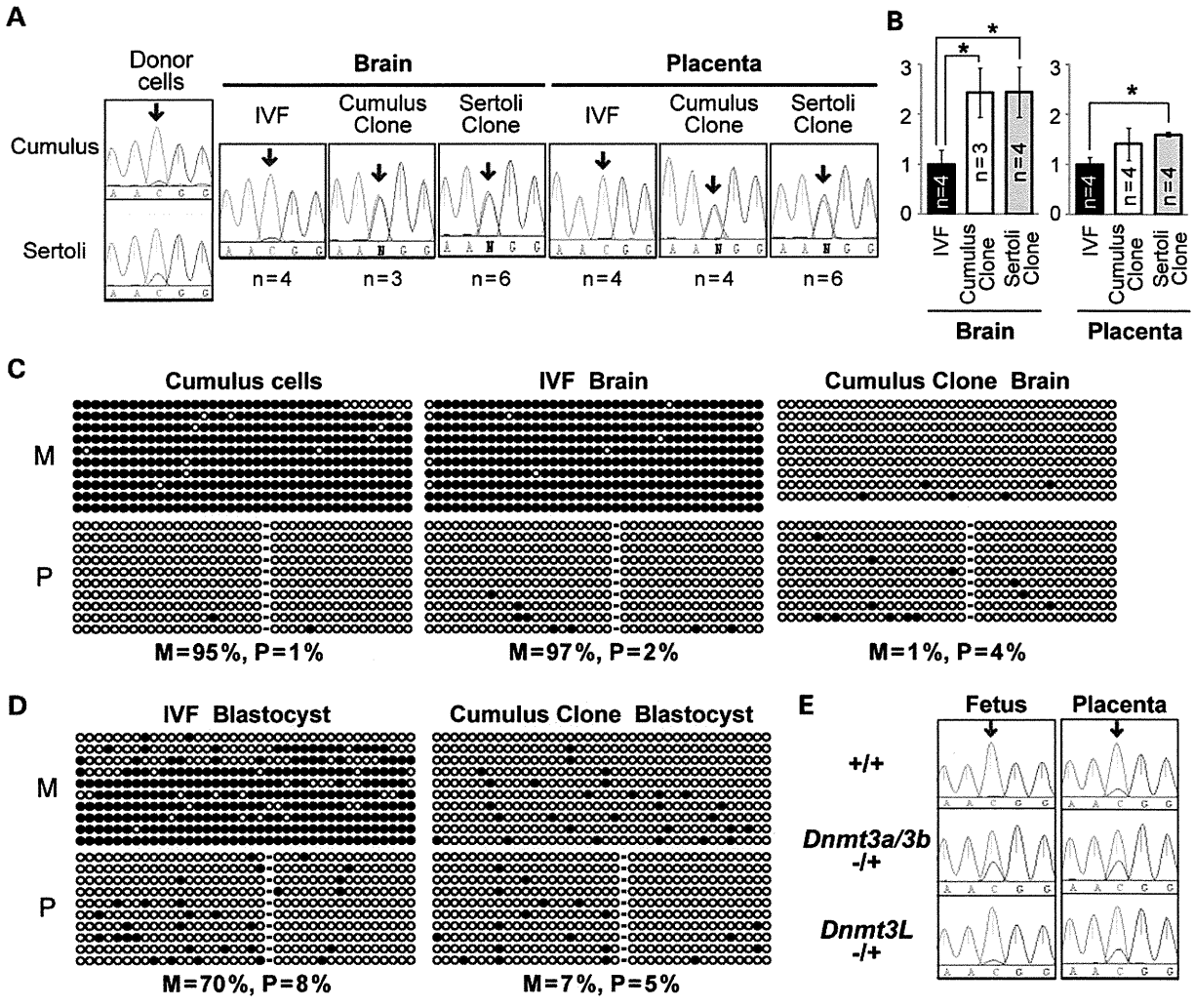


**Figure 3.** Consistent loss of *Slc38a4* imprinting in cloned mice. (**A**) Allelic expression of *Slc38a4*. *Slc38a4* showed paternal expression in IVF-derived samples but showed biallelic expression in all cloned mouse brains and placentas analyzed. The numbers of analyzed samples are shown. Very similar data were obtained for all cloned samples. (**B**) Real-time RT–PCR analysis of *Slc38a4*. The mean expression level of the IVF-derived samples is set as 1. The error bars indicate means ± SD of three or four samples. $^*P < 0.05$ (Student's *t*-test). (**C**) DNA methylation analysis of the *Slc38a4* DMR in cumulus cells and brains. Black and white circles indicate methylated and unmethylated residues. The percentages of methylated CpG sites of the maternal allele (M) and the paternal allele (P) are indicated. (**D**) DNA methylation analysis of the *Slc38a4* DMR in cloned blastocysts. (**E**) Allelic expression of *Slc38a4* in the concepti obtained from *Dnmt3L*-deficient and oocyte-specific *Dnmt3a/3b*-deficient females.

expression of *Dlk1* was observed in two of four cloned mouse placentas produced without TSA treatment (Supplementary Material, Fig. S4G). These data indicated that loss of *Gab1*, *Sfmbt2*, *Slc38a4* and *Dlk1* imprinting was caused by SCNT, not by TSA treatment.

### Characteristics of genes with consistent loss of imprinting in cloned mice

As described earlier, *Gab1*, *Sfmbt2* and *Slc38a4* showed consistent loss of imprinting in cloned mice. These three genes were all maternally repressed and did not require *de novo* DNA methylation in growing oocytes for the establishment of imprinting (Table 1). No paternally methylated germline DMR has been found near these genes in the recent whole-genome DNA methylation analysis of germ cells (23). Importantly, these genes showed normal expression levels in the placentas of bi-maternal embryos that contained genomes from non-growing and fully grown oocytes (Table 1 and (28)). If a paternally expressed gene is not regulated by maternal imprinting, it is repressed in bi-maternal embryos (Supplementary Material, Fig. S7A). For example, *Igf2* and *Dlk1*, which are paternally expressed and regulated by paternal imprinting, showed greatly reduced expression in bi-maternal embryos compared with wild-type embryos (Table 1). These data suggest that imprinting of *Gab1*, *Sfmbt2* and *Slc38a4* may be

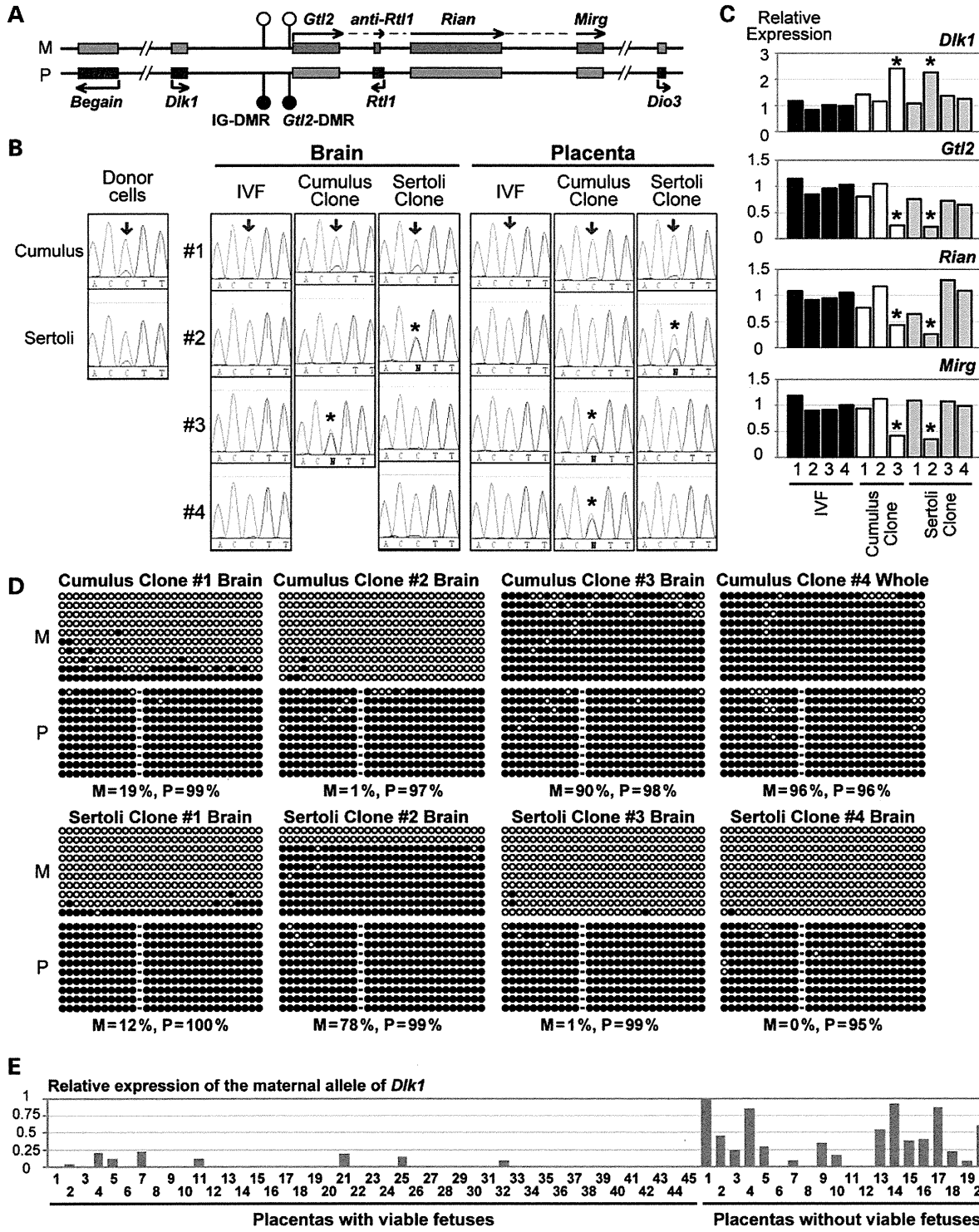


**Figure 4.** Loss of *Dlk1-Dio3* imprinting and embryonic lethality in cloned mice. (**A**) Genomic structure of the *Dlk1-Dio3* domain. Maternally expressed genes and paternally expressed genes are in red and blue, respectively. Open circles and filled circles indicate unmethylated and methylated DMRs, respectively. M, maternal allele; P, paternal allele. (**B**) Allelic expression of *Dlk1*. Biallelic expression is marked with an asterisk. For cumulus clone #4, the brain sample was not analyzed because of severe growth retardation of this clone. (**C**) Real-time RT–PCR analysis of *Dlk1*, *Gtl2*, *Rian* and *Mirg* in the brain. The mean expression level of the

**Table 1.** Unique characteristics of Gab1, Sfmbt2 and Slc38a4

| Gene | Frequency of loss of imprinted expression | *de novo* DNA methylation in growing oocytes | Expression in bi-maternal placentas (fold decrease) |
|---|---|---|---|
| *Gab1* | 14/14[a] | Not required(19) | 1.38 ± 0.12 |
| *Sfmbt2* | 14/14[a] | Not required(19) | 1.31 ± 0.39 |
| *Slc38a4* | 14/14[a] | Not required | 1.07 ± 0.15 |
| *Igf2* | 0/8 | Not required[$b] | 37.9 ± 14.8[c] |
| *Dlk1* | 5/12 | Not required[$b] | 24.5 ± 5.4[c] |
| *Peg10* | 0/8 | Required[$b] | 1.03 ± 0.22 |
| *Mest* | 1/8 | Required[$b] | 1.38 ± 0.47 |
| *Peg3* | 0/8 | Required[$b] | 1.13 ± 0.15 |

Paternally expressed genes known to be regulated by DNA methylation during spermatogenesis (*Igf2* and *Dlk1*) and oogenesis (*Peg10*, *Mest* and *Peg3*) are included for comparison. The frequency of loss of imprinted expression is based on results obtained using E13.5 cloned mouse placentas. Microarray data of bi-maternal placentas (28) are used for the calculation of the fold decrease (means ± SD from three replicates).
[a]Statistically significant compared with IVF embryos ($P < 0.05$, Fisher's exact test).
[$b]See Supplementary Material, Figure S7B.
[c]Statistically significant compared with control placentas ($P < 0.05$, Student's *t*-test).

established during oocyte growth in a *de novo* DNA methylation-independent manner.

## DISCUSSION

### Relationships between developmental abnormalities and imprinting defects in cloned mice

We found a correlation between embryonic lethality and loss of *Dlk1-Dio3* imprinting. Loss of *Dlk1-Dio3* imprinting in cloned mice was caused by the paternalization of the maternal allele, which is very similar to the maternal transmission of IG-DMR knockout allele (ΔIG-DMR/+). While ΔIG-DMR/+ fetuses are perinatal lethal and show muscle and skeletal defects at late gestational stage, the overall growth performance is normal (24). On the other hand, cloned fetuses with loss of *Dlk1-Dio3* imprinting were absorbed by term, and muscle and skeletal defects at late gestational stage thus cannot be analyzed. While the underlying mechanism of the fetal absorption is unclear, these data suggest that the combination of loss of *Dlk1-Dio3* imprinting and other abnormalities may cause earlier embryonic death in cloned mice. Loss of *Dlk1-Dio3* imprinting is also observed in various induced pluripotent stem cell (iPSC) lines (29), highlighting the similarity of two reprograming strategies, SCNT and iPSC production. It has not yet been determined why loss of *Dlk1-Dio3* imprinting occurs in cloned mice and iPSCs. However, it is reported that high expression of Oct4 and Klf4 combined with lower expression of c-Myc and Sox2 prevents loss of *Dlk1-Dio3* imprinting in iPSCs (30). Cloned mouse embryos frequently show reduced or ectopic expression of Oct4 during the preimplantation stage (31), and it is possible that abnormal expression of Oct4 induces loss of *Dlk1-Dio3* imprinting in cloned mice.

Placentomegaly is observed in all cloned mouse concepti (3). *Sfmbt2* is the only known protein-coding gene in proximal chromosome 2. The paternal duplication of proximal chromosome 2, which causes overexpression of *Sfmbt2*, is known to result in placentomegaly (32). In contrast, deficiency of *Gab1* is known to result in the reduction of placental size (33). The overexpression of *Sfmbt2* and *Gab1* observed in cloned placentas might be involved in placentomegaly of cloned mice. It is also proposed that imprinted expression of *Slc38a4* in the placenta may be important for the normal supply of neutral amino acids to the fetus (34). Thus *Slc38a4*-knockout or -transgenic mice, which have not been reported, merit further investigation to understand the phenotypic abnormalities of cloned animals.

While we focused on imprinted genes in this study, many non-imprinted genes were also reported to show aberrant expression in cloned mice, especially in the placenta (35). Aberrant expression of both imprinted genes and non-imprinted genes may impact the size and viability of cloned mouse embryos.

### Consistent loss of imprinting caused by incomplete imprinting memory in somatic cells

Two placenta-specific imprinted genes, *Gab1* and *Sfmbt2*, showed complete loss of imprinting in all cloned placentas analyzed. In the donor cells, neither gene showed imprinted expression. In the promoter region, allele-specific DNA methylation of *Gab1* and allelic enrichment of histone modifications of *Sfmbt2* were not observed in donor cells or cloned placentas. These data suggested that the imprinting of *Gab1* and *Sfmbt2* was not retained in somatic cells and not reinstated in the placental lineages derived from cloned somatic cells.

In addition to *Gab1* and *Sfmbt2*, there are several additional genes that show tissue-specific imprinted expression. We found that four placenta-specific and three brain-specific imprinted genes showed normal monoallelic expression in the cloned mice. These seven genes are all present within imprinted gene clusters that have germline DMRs, but *Gab1* and *Sfmbt2* are not. It is likely that monoallelic expression of these seven tissue-specific imprinted genes was reestablished after SCNT, using imprinting marks retained in the clusters.

*Slc38a4* shows imprinted expression both in the normal fetus and placenta (22), and imprinted methylation at the *Slc38a4* DMR was maintained in the donor cells. However, the *Slc38a4* DMR of somatic cells was not protected from demethylation during preimplantation development. Interestingly, paternal expression of *Slc38a4* was not lost in embryos obtained from *Dnmt3L*-deficient and oocyte-specific *Dnmt3a/3b*-deficient female mice. Therefore, we hypothesize that, during oogenesis,

IVF-derived samples is set as 1. Samples with biallelic expression of *Dlk1* are marked with an asterisk. (**D**) DNA methylation analysis of the IG-DMR by bisulfite sequencing in cloned mouse brains. The DNA methylation of cumulus clone #4 was analyzed in the whole fetus. The percentages of methylated CpG sites are indicated. (**E**) Summary of allelic expression of *Dlk1* in term placentas from a series of experiments using *Xist*-siRNA (see Supplementary Material, Table S2 for details). Donor cells were collected from [B6xDBA]F1 mice. The expression level of the maternal allele of *Dlk1* is normalized by that of the paternal allele. Forty-five placentas with viable fetuses and 20 placentas without viable fetuses (the fetus of #11 was small and dead, and the other fetuses were absorbed) were analyzed. Increased expression of the maternal allele of *Dlk1* is observed in the placentas without viable fetuses ($P < 10^{-9}$, Student's *t*-test).